Engineering Robust and Functional Vascular Networks In Vivo With Human Adult and Cord Blood Derived Progenitor Cells

Juan M. Melero-Martin, Maria E. De Obaldia, Soo-Young Kang, Zia A. Khan, Lei Yuan, Peter Oettgen and Joyce Bischoff

Circ. Res. 2008;103;194-202; originally published online Jun 12, 2008;
DOI: 10.1161/CIRCRESAHA.108.178590
Circulation Research is published by the American Heart Association. 7272 Greenville Avenue, Dallas, TX 72514
 Print ISSN: 0009-7330. Online ISSN: 1524-4571

Engineering Robust and Functional Vascular Networks In Vivo With Human Adult and Cord Blood–Derived Progenitor Cells

Juan M. Melero-Martin, Maria E. De Obaldia, Soo-Young Kang, Zia A. Khan, Lei Yuan, Peter Oettgen, Joyce Bischoff

Abstract—The success of therapeutic vascularization and tissue engineering will rely on our ability to create vascular networks using human cells that can be obtained readily, can be expanded safely ex vivo, and can produce robust vasculogenic activity in vivo. Here we describe the formation of functional microvascular beds in immunodeficient mice by coimplantation of human endothelial and mesenchymal progenitor cells isolated from blood and bone marrow. Evaluation of implants after 1 week revealed an extensive network of human blood vessels containing erythrocytes, indicating the rapid formation of functional anastomoses within the host vasculature. The implanted endothelial progenitor cells were restricted to the luminal aspect of the vessels; mesenchymal progenitor cells were adjacent to lumens, confirming their role as perivascular cells. Importantly, the engineered vascular networks remained patent at 4 weeks in vivo. This rapid formation of long-lasting microvascular networks by postnatal progenitor cells obtained from noninvasive sources constitutes an important step forward in the development of clinical strategies for tissue vascularization. (***Circ Res*****. 2008;103:194-202.)**

Key Words: vascular networks ■ endothelial progenitor cells ■ mesenchymal stem cells ■ mesenchymal progenitor cells ■ tissue engineering ■ regenerative medicine ■ vasculogenesis ■ angiogenesis

Engineered tissues must have the capacity to generate a vascular network that rapidly forms anastomoses with the host vasculature to guarantee adequate nutrients, gas exchange, and elimination of waste products.[1] Presently, there are no tissue-engineered (TE) constructs clinically available with an inherent microvascular bed, and therefore successes have been restricted to the replacement of relatively thin (skin) or avascular (cartilage) tissues, where postimplantation vascularization from the host is sufficient.

To overcome the problem of vascularization, strategies to promote ingrowth of microvessels by delivery of angiogenic molecules have been proposed.[2–5] However, rapid and complete vascularization of thick engineered tissues is likely to require an additional process of vasculogenesis.[1,6] Toward this goal, the feasibility of engineering microvascular networks in vivo has been shown using human umbilical vein endothelial cells and human microvascular endothelial cells[7–9]; however, such autologous tissue-derived endothelial cells (ECs) present problems for wide clinical use, because they are difficult to obtain in sufficient quantities. These limitations have instigated the search for other sources of ECs, such as those derived from embryonic and adult stem and progenitor cells.[6] For instance, ECs derived from embryonic stem cells (ESCs) have been used to form blood vessels and to enhance the vascularization of engineered skeletal muscle constructs in vivo.[10,11] However, the mechanisms controlling ESCs differentiation must be understood, and ethical issues surrounding their use must be resolved before their implementation in therapeutic strategies.

The identification of endothelial progenitor cells (EPCs) in blood presented an opportunity to noninvasively obtain ECs.[12–14] We and other authors have shown that adult and cord blood–derived EPCs have the required vasculogenic capacity to form functional vascular networks in vivo.[15–17] Importantly, these studies have also shown that to obtain stable and durable vascular networks, EPCs require coimplantation with perivascular cells. In our previous work, the role of perivascular cells was undertaken by smooth muscle cells (SMCs) isolated from human saphenous veins.[15] In the work by Au et al, the mouse embryonic cell line 10T1/2 served as the perivascular component of the vascular networks.[16] However, neither source is suitable for clinical utilization: harvesting SMCs from healthy vasculature would impose serious morbidity in patients and murine-derived cell lines will not be used in humans. Therefore, to exploit the full vasculogenic potential of EPCs, we set out to establish

Original received April 29, 2008; revision received May 29, 2008; accepted May 30, 2008.

From the Vascular Biology Program and Department of Surgery, Children's Hospital Boston (J.M.M.-M., M.E.D.O., S.-Y.K., Z.A.K., J.B.); and Division of Cardiology, Beth Israel Deaconess Medical Center (L.Y., P.O.), Harvard Medical School, Boston Mass.

Correspondence to Dr Joyce Bischoff, Vascular Biology Program and Department of Surgery, Children's Hospital Boston, Harvard Medical School, Boston, MA 02115. E-mail joyce.bischoff@childrens.harvard.edu

Circulation Research **is available at http://circres.ahajournals.org** **DOI: 10.1161/CIRCRESAHA.108.178590**

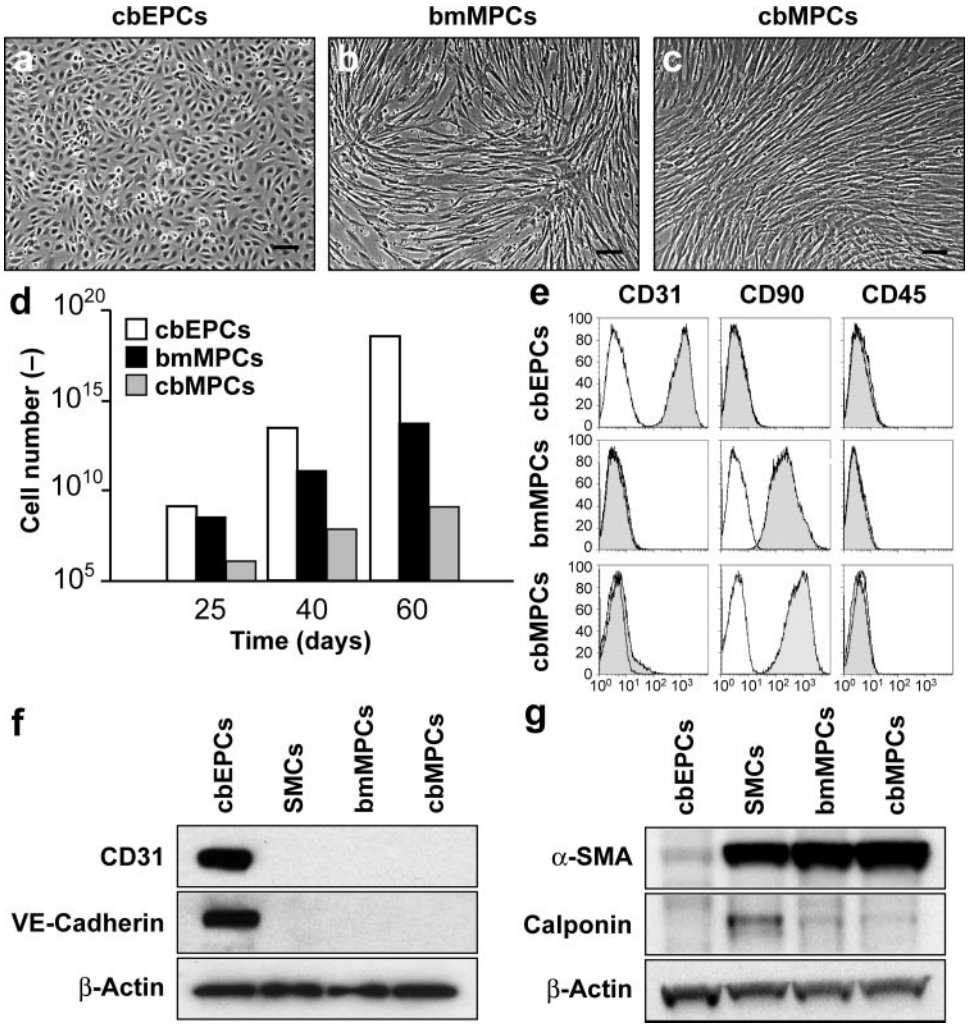

Figure 1. Phenotypic characterization of EPCs and MPCs. a through c, cbEPCs presented typical cobblestone morphology (a), whereas both bmMPCs (b) and cbMPCs (c) presented spindle morphology characteristic of mesenchymal cells in culture. Scale bars=100 μm. d, cbEPCs and MPCs were serially passaged and their in vitro expansion potential estimated by the accumulative cell numbers obtained from 25 mL of either cord blood or bone marrow samples. e, Flow cytometric analysis of cbEPCs, bmMPCs, and cbMPCs for the endothelial marker CD31, mesenchymal marker CD90, and hematopoietic marker CD45. Solid gray histograms represent cells stained with fluorescent antibodies. Isotype-matched controls are overlaid in a black line on each histogram. f and g, Western blot analyses of cbEPCs, bmMPCs, and cbMPCs for endothelial markers CD31 and VE-cadherin (f) and mesenchymal markers α-SMA and calponin (g). Expression of β-actin shows equal protein loading. SMCs isolated from human saphenous vein served as control.

clinically viable sources of perivascular cells. The ideal perivascular cells must present several key properties: (1) isolation with minimal donor site morbidity; (2) availability in sufficient quantities; and (3) immunologic compatibility with the recipients.[1] Mesenchymal stem/progenitor cells (herein referred to as MPCs)[18] meet these requirements. MPCs can be isolated by minimally invasive procedures from a diversity of human tissues, including bone marrow,[18] adult blood,[19] umbilical cord blood,[20–22] and adipose tissue.[23] Furthermore, MPCs undergo self-renewal and therefore can potentially be expanded to sufficient quantities for tissue and organ regeneration.[24]

Here, we demonstrate that MPCs obtained from both human adult bone marrow and human cord blood can serve as perivascular cells for in vivo vasculogenesis. Subcutaneous coimplantation of EPCs and MPCs, suspended as single cells in Matrigel, into immunodeficient mice resulted in the creation of extensive microvascular beds that rapidly formed anastomoses with the host vasculature. This study constitutes a step forward in the clinical development of therapeutic vasculogenesis by showing the feasibility of using human adult and cord blood–derived progenitor cells as the basic cellular building blocks to create functional vascular networks in vivo.

Materials and Methods

In Vivo Vasculogenesis Assay

The formation of vascular networks in vivo was evaluated using a xenograft model as described.[15] A total of 1.9×10^6 cells was resuspended in 200 μL of ice-cold Phenol Red-free Matrigel (BD Bioscience, San Jose, Calif), at ratios of 100:0, 80:20, 60:40, 40:60, 20:80, and 0:100 (EPCs:MPCs). The mixture was implanted on the back of a 6-week-old male athymic nu/nu mouse (Massachusetts General Hospital, Boston, Mass) by subcutaneous injection using a 25-gauge needle. Implants of Matrigel alone served as controls. One implant was injected per mouse. Each experimental condition was performed with 4 mice. Animal experiments were conducted under a protocol approved by the Institutional Animal Care and Use Committee at Children's Hospital Boston in an AAALAC-approved facility.

An expanded Materials and Methods section, available at http://circres.ahajournals.org, describes cell isolation and expansion, flow cytometry, Western blot analysis, differentiation assays, histology and immunohistochemistry, retroviral transduction, luciferase assay, microvessel density evaluation, and statistical analysis.

Results

Isolation of EPCs and MPCs

Cord blood–derived (cb)EPCs (Figure 1a) and adult blood (ab)EPCs were isolated from the mononuclear cells fraction of human blood samples and purified by CD31 selection as

described (see supplemental Figures I and XII in online the online data supplement for morphology of cbEPCs and abEPCs, respectively).[15] MPCs were isolated from the mononuclear cells fractions of human bone marrow samples (bmMPCs) and human cord blood samples (cbMPCs). bmMPCs adhered rapidly to the culture plates and proliferated until confluent, whereas cbMPCs emerged more slowly, forming mesenchymal-like colonies after one week (supplemental Figure I). cbMPC colonies were selected with cloning rings and expanded. Both bmMPCs (Figure 1b) and cbMPCs (Figure 1c) presented spindle morphology characteristic of mesenchymal cells in culture.[18]

cbEPCs and MPCs were grown in EPC medium and MPC medium, respectively, and their expansion potentials estimated by the cumulative cell numbers obtained from 25 mL of either cord blood or bone marrow samples after 25, 40, and 60 days in culture (Figure 1d). Remarkably, up to 10^{13} cbEPCs and 10^{11} bmMPCs were obtained after 40 days, consistent with previous studies.[13,15] The number of cells continued to increase so that at 60 days, there were an estimated 10^{18} cbEPCs and 10^{14} bmMPCs, respectively. In the case of cbMPCs, a longer culture period was necessary to obtain such numbers. The apparent decreased number of cbMPCs was likely attributable to the smaller number of MPCs in cord blood samples (typically 1 to 2 colonies per 25 mL; data not shown) as compared with bone marrow samples, where the majority of the adherent cells contributed to the final bmMPC population (supplemental Figure I).

The phenotype of the MPCs was confirmed by 3 methods. Flow cytometry (Figure 1e) showed that bmMPCs and cbMPCs uniformly expressed the mesenchymal marker CD90 and were negative for the endothelial marker CD31 and the hematopoietic marker CD45 (see further flow cytometric evaluations in supplemental Figure II). cbEPCs served as a control. Western blot analyses (Figure 1f and 1g) confirmed the mesenchymal phenotype of bmMPCs and cbMPCs (expression of α-smooth muscle actin [SMA] and calponin) and the endothelial phenotype of cbEPCs (expression of CD31 and VE-cadherin). These data were extended by indirect immunofluorescent staining (supplemental Figure III): bmMPCs and cbMPCs were shown to express the mesenchymal markers α-SMA, calponin, and NG_2 but not the EC markers CD31, VE-cadherin, and von Willebrand factor. Importantly, smooth muscle myosin heavy chain (smMHC), a specific marker of differentiated smooth muscle cells,[25,26] was found in mature SMCs but not in any of the MPCs.

The ability of MPCs to differentiate into multiple mesenchymal lineages was evaluated in vitro using well-established protocols.[18] Both bmMPCs and cbMPCs differentiated into osteocytes and chondrocytes, as shown by the expression of alkaline phosphatase (osteogenesis; Figure 2a and 2b) and glycosaminoglycan deposition in pellet cultures (chondrogenesis; Figure 2c and 2d), respectively (see also supplemental Figure IV). Adipogenesis was only evident with bmMPCs (Figure 2e) and not in cbMPCs (Figure 2f). This loss of adipogenic potential, reported for other mesenchymal cells in culture,[27,28] was attributed to the extensive expansion that these cells required because of their lower presence in cord

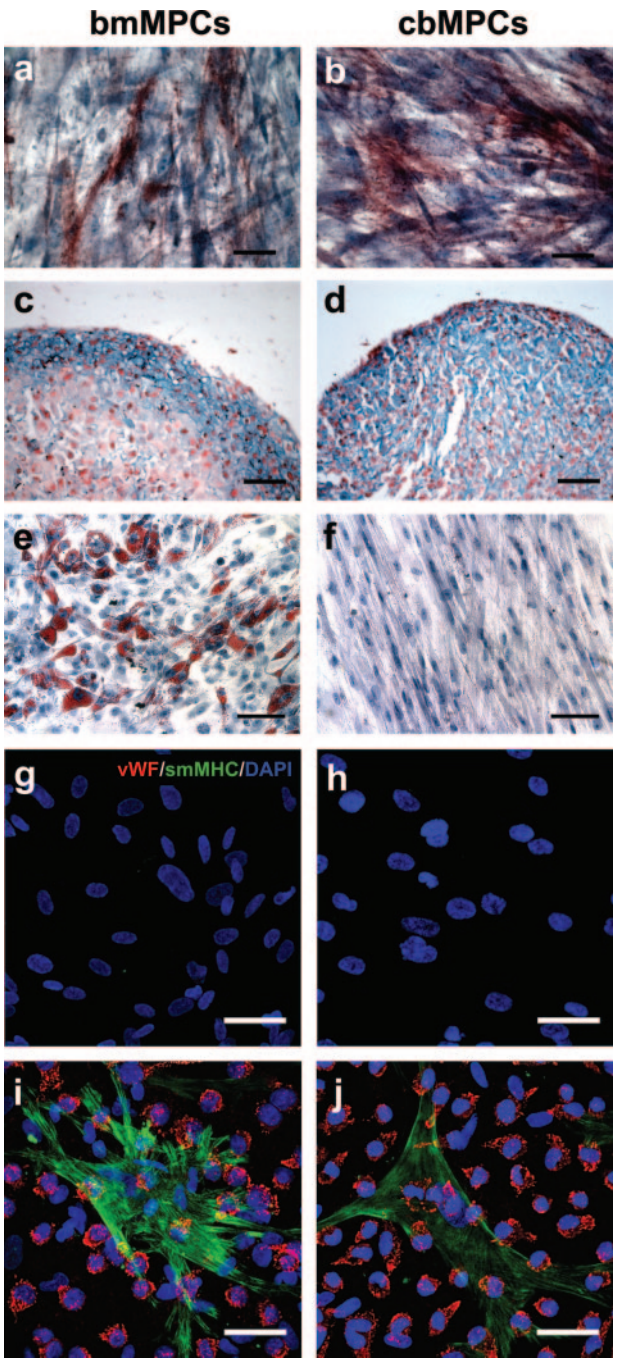

Figure 2. Multilineage differentiation of MPCs. a and b, bmMPC (a) and cbMPC (b) differentiation into osteocytes was revealed by alkaline phosphatase staining. c and d, bmMPC (c) and cbMPC (d) differentiation into chondrocytes was revealed by the presence of glycosaminoglycans, detected by Alcian blue staining. The presence of adipocytes was assessed by oil red O staining, and it was evident in bmMPCs (e) but absent in cbMPCs (f). Smooth muscle cell differentiation was evaluated by culturing MPCs in the absence or presence of cbEPCs (1:1 EPC-to-MPC ratio) for 7 days in EPC medium. Induction of SMC phenotype was assessed by the expression of smMHC. Immunofluorescence staining with anti–von Willebrand factor–Texas red and anti–smMHC-FITC, as well as nuclear staining with DAPI, revealed that smMHC was absent in both bmMPCs (g) and cbMPCs (h), but it was induced in MPCs when cocultured with cbEPCs (i and j). Scale bars correspond to 200 μm (e and f) and 50 μm (a through d and g through j).

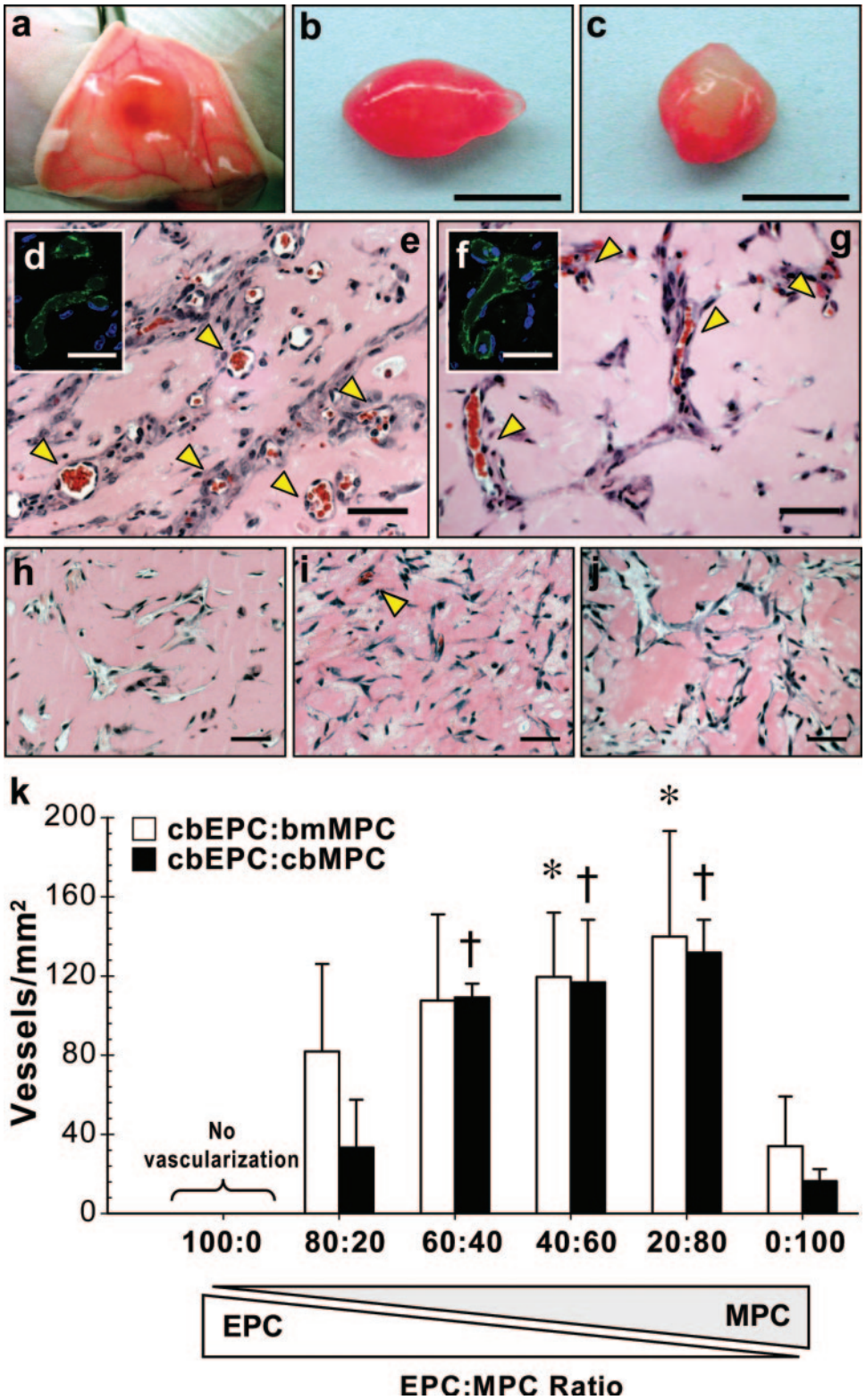

Figure 3. Formation of vascular networks in vivo with EPCs and MPCs. A total of 1.9×10^6 cells was resuspended in 200 μL of Matrigel using different ratios of cbEPCs and MPCs and implanted on the backs of 6-week-old nu/nu mice by subcutaneous injection. Implants were harvested after 7 days and stained with H&E. a through c, Macroscopic view of explanted Matrigel plugs seeded with 40% cbEPCs:60% bmMPCs (a and b) and 40% cbEPCs:60% cbMPCs (c). Scale bars=5 mm. e, g, and h through j, H&E staining revealed the presence of lumenal structures containing erythrocytes (yellow arrow heads) in implants where both cells types (cbEPCs and MPCs; 40:60) were used (e and g) but not in implants where cbEPCs (h), bmMPCs (i), and cbMPCs (j) were used alone. Scale bars=50 μm. d and f, Microvessels stained positive for human CD31. Scale bars=30 μm. Images are representative of implants harvested from at least 4 different mice. k, Quantification of microvessel density was performed by counting erythrocyte-filled vessels in implants with ratios of 100:0, 80:20, 60:40, 40:60, 20:80, and 0:100 (cbEPCs:MPCs; n≥4 each condition). Each bar represents the mean±SD (vessels/mm^2) obtained from vascularized implants. *$P<0.05$ compared with implants with bmMPCs alone (n=4); †$P<0.05$ compared with implants with cbMPCs alone (n=4).

blood samples (the earliest cbMPCs were tested for adipogenesis was at passage 5).

Because we intended to test MPCs as perivascular cells to engineer microvessel networks, we evaluated the ability of MPCs to differentiate toward a smooth muscle phenotype. As already shown, MPCs and mature SMCs shared a number of cellular markers including α-SMA, calponin, NG_2, and platelet-derived growth factor receptor-β (supplemental Figure V). Although the definitive smooth muscle cell marker smMHC was absent in MPCs (Figure 2g and 2h), both bmMPCs and cbMPCs were induced to express smMHC when directly cocultured with cbEPCs (Figure 2i and 2j). Importantly, induction did not occur when MPCs were indirectly cocultured with cbEPCs using a Transwell culture system (supple-

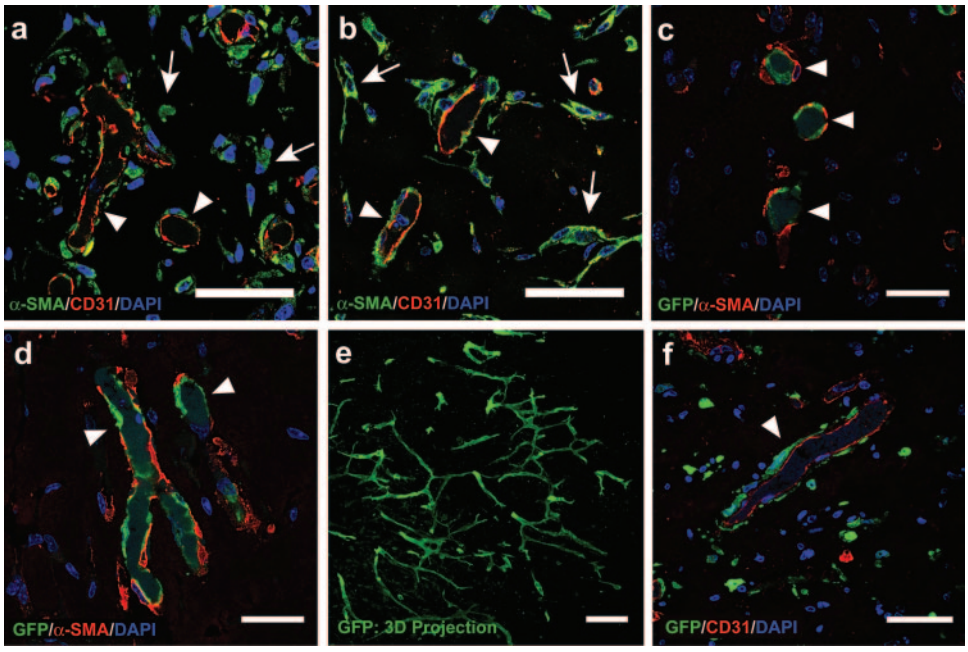

Figure 4. Specific location of EPCs and MPCs in the vascular bed. Matrigel implants containing cbEPCs and MPCs (40:60) were evaluated after 1 week. a and b, Implants with bmMPCs (a) and cbMPCs (b) produced lumenal structures that stained positive for human CD31, confirming that those lumens were formed by the implanted cells. In addition, α-SMA–expressing cells were detected both in the proximity (white arrows) and around the lumenal structures (white arrow heads). Scale bars=50 μm. c and d, Implants that used GFP-labeled cbEPC and either bmMPCs (c) or cbMPCs (d) produced GFP-positive lumenal structures (white arrow heads) covered by α-SMA–expressing perivascular cells, confirming that cbEPCs were restricted to the luminal aspect of the vessels. Scale bars=30 μm. e, Projections of whole-mount staining showed that the GFP-expressing cells formed extensive networks throughout the implants. Scale bar=100 μm. f, Implants that used GFP-labeled bmMPC and unlabeled cbEPCs resulted in human CD31-positive lumenal structures with GFP-expressing cells adjacent to lumens (white arrow heads), confirming the role of MPCs as perivascular cells. Scale bars=50 μm. Images are representative of implants harvested from 4 different mice.

mental Figure VI), consistent with previous reports that showed direct contact with ECs is required for mesenchymal cell differentiation into SMCs.[29,30]

In Vivo Formation of Human Vascular Networks

We have previously demonstrated the vasculogenic capacity of blood-derived EPCs both in vitro and in vivo.[15,31] In these studies, the presence of vascular smooth muscle cells was required for formation of vascular networks. To answer the question of whether MPCs could be used instead of SMCs, we implanted different combinations of cbEPCs and MPCs (either bmMPCs or cbMPCs) into nude mice for 1 week (Figure 3). A total of 1.9×10^6 cells was resuspended in 200 μL of Matrigel, using ratios of 100:0, 80:20, 60:40, 40:60, 20:80, and 0:100 (percentage of cbEPCs:percentage of MPCs) and injected subcutaneously. After harvesting the Matrigel implants (Figure 3a through 3c), hematoxylin/eosin (H&E) staining revealed numerous vessels containing erythrocytes in implants containing both cbEPCs and MPCs (Figure 3e and 3g). The structures stained positive for human CD31 (Figure 3d and 3f), confirming the lumens were lined by the implanted cells (the specificity of the antihuman CD31 antibody is shown in supplemental Figure IX). Implants of Matrigel alone were devoid of vessels (supplemental Figure VII), indicating the Matrigel itself was not responsible for the presence of vascular structures. As expected,[15] implants with cbEPCs alone (Figure 3h) failed to form microvessels. Implants with only MPCs (Figure 3i and 3j) presented infiltration of murine blood capillaries but no human microvessels (supplemental Figure IX). The ability of human MPCs to recruit murine vessels into Matrigel may be explained by the secretion of vascular endothelial growth factor (VEGF) from MPCs but not cbEPCs (supplemental Figure VIII).

Microvessel density was determined by quantification of lumens containing red blood cells (Figure 3k). The extent of the engineered vascular networks was influenced by the ratio of EPCs to MPCs (Figure 3k). A progressive increase in MPCs resulted in increased microvessel density and more consistent vascularization (supplemental Table I). When the ratio of EPC:MPC was 40:60, an average density of 119 ± 33 and 117 ± 32 vessels/mm^2 with bmMPCs or cbMPCs, respectively, was achieved in all implants. These densities were significantly higher ($P<0.05$) than those observed with MPCs alone, reaffirming the necessity of the endothelial component for the formation of human vessels in the implants.

Assembly of Endothelial and Mesenchymal Progenitor Cells in the Vascular Bed

In addition to the human CD31-positive lumenal structures, the engineered vessels were characterized by α-SMA staining of perivascular cells (Figure 4a and 4b). With bmMPCs or cbMPCs, α-SMA–positive cells were detected both in proximity and adjacent to lumenal structures, suggesting an ongoing process of perivascular cell recruitment during vessel maturation.[32–34] To determine more precisely the contribution of each cell type, we implanted green fluorescent protein (GFP)-labeled cbEPCs with unlabeled MPCs. Anti-GFP staining showed cbEPCs restricted to lumenal positions in the microvessel networks, whereas anti–α-SMA staining showed that the GFP-labeled vessels were covered by perivascular cells; this observation was valid with both sources of MPCs (Figure 4c and 4d). Projections of whole-mount staining showed that the GFP-expressing cells formed

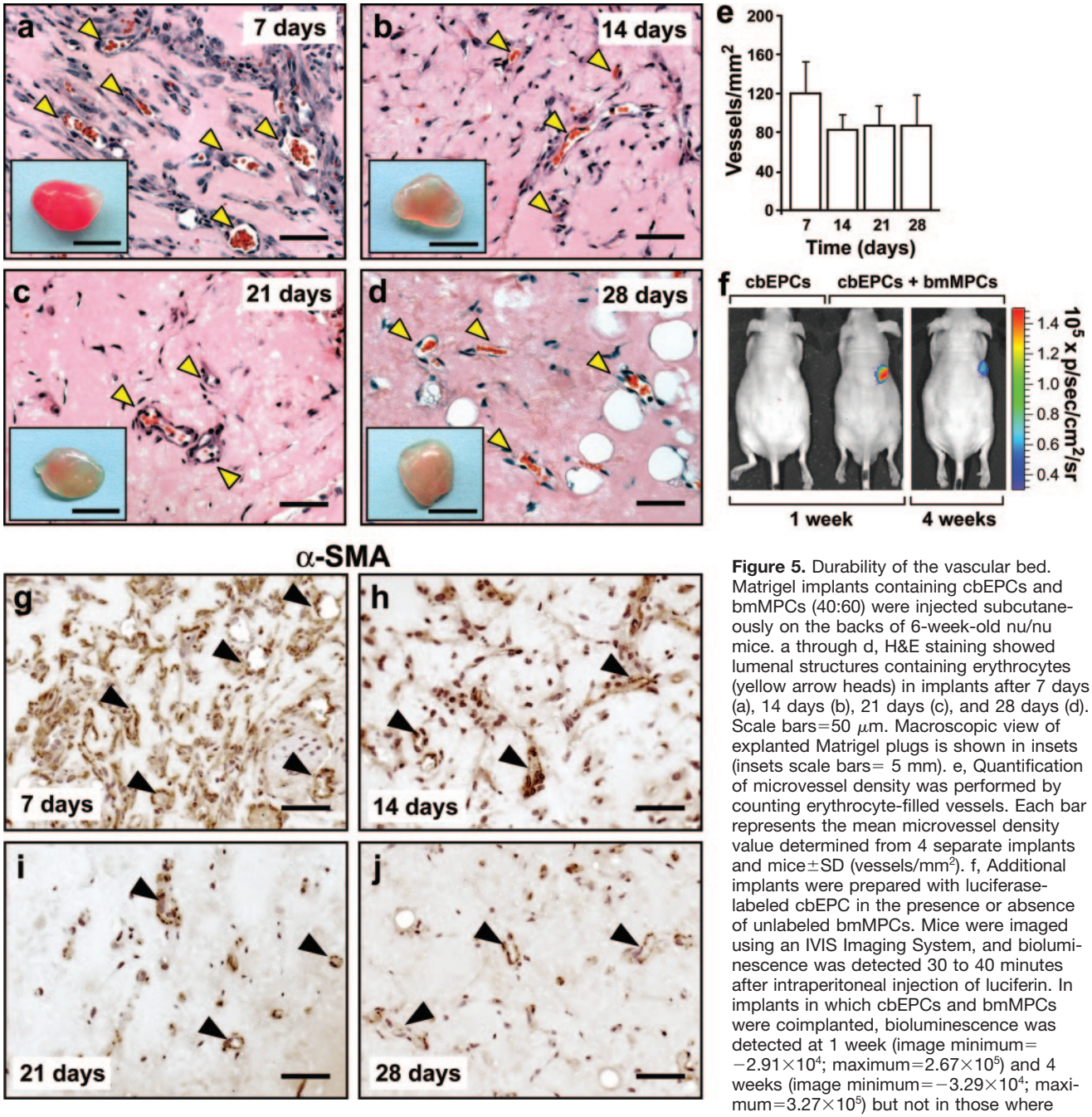

Figure 5. Durability of the vascular bed. Matrigel implants containing cbEPCs and bmMPCs (40:60) were injected subcutaneously on the backs of 6-week-old nu/nu mice. a through d, H&E staining showed lumenal structures containing erythrocytes (yellow arrow heads) in implants after 7 days (a), 14 days (b), 21 days (c), and 28 days (d). Scale bars=50 μm. Macroscopic view of explanted Matrigel plugs is shown in insets (insets scale bars= 5 mm). e, Quantification of microvessel density was performed by counting erythrocyte-filled vessels. Each bar represents the mean microvessel density value determined from 4 separate implants and mice±SD (vessels/mm^2). f, Additional implants were prepared with luciferase-labeled cbEPC in the presence or absence of unlabeled bmMPCs. Mice were imaged using an IVIS Imaging System, and bioluminescence was detected 30 to 40 minutes after intraperitoneal injection of luciferin. In implants in which cbEPCs and bmMPCs were coimplanted, bioluminescence was detected at 1 week (image minimum=-2.91×10^4; maximum=2.67×10^5) and 4 weeks (image minimum=-3.29×10^4; maximum=3.27×10^5) but not in those where cbEPCs were used alone. g through j, Immunohistochemical staining of α-SMA in implants after 7 days (g), 14 days (h), 21 days (i), and 28 days (j) revealed that α-SMA–expressing cells were progressively restricted to perivascular locations (black arrow heads). Scale bars=50 μm. Images are representative of implants harvested from 4 different mice.

extensive networks throughout the implants (Figure 4e). Conversely, we implanted GFP-labeled bmMPCs with unlabeled cbEPCs to identify input MPCs without relying on anti–α-SMA. Sections were stained with anti-GFP and anti-CD31 antibodies: GFP-expressing cells were detected as perivascular cells surrounding human CD31$^+$ lumens and as individual cells dispersed throughout the Matrigel implants (Figure 4f).

Durability of the Vascular Bed

To test the durability of the engineered vascular beds in vivo, we evaluated implants of cbEPCs/bmMPCs (40:60) at 7, 14, 21, and 28 days after xenografting (Figure 5). H&E staining revealed the presence of lumenal structures containing erythrocytes in all implants at each time point (Figure 5a through 5d). Microvessel quantification (Figure 5e) revealed an initial reduction (statistically nonsignificant; $P=0.105$) in the number of patent blood vessels from 119±33 vessels/mm^2 at day 7 to 83±16 vessels/mm^2 at day 14. Microvessel densities remained stable thereafter (87±21 and 87±32 vessels/mm^2 at days 21 and 28, respectively).

To further evaluate the engineered vascular bed, we used a luciferase-based imaging system to monitor perfusion of the Matrigel implants. cbEPCs were infected with lentivirus-associated vector encoding luciferase and implanted into

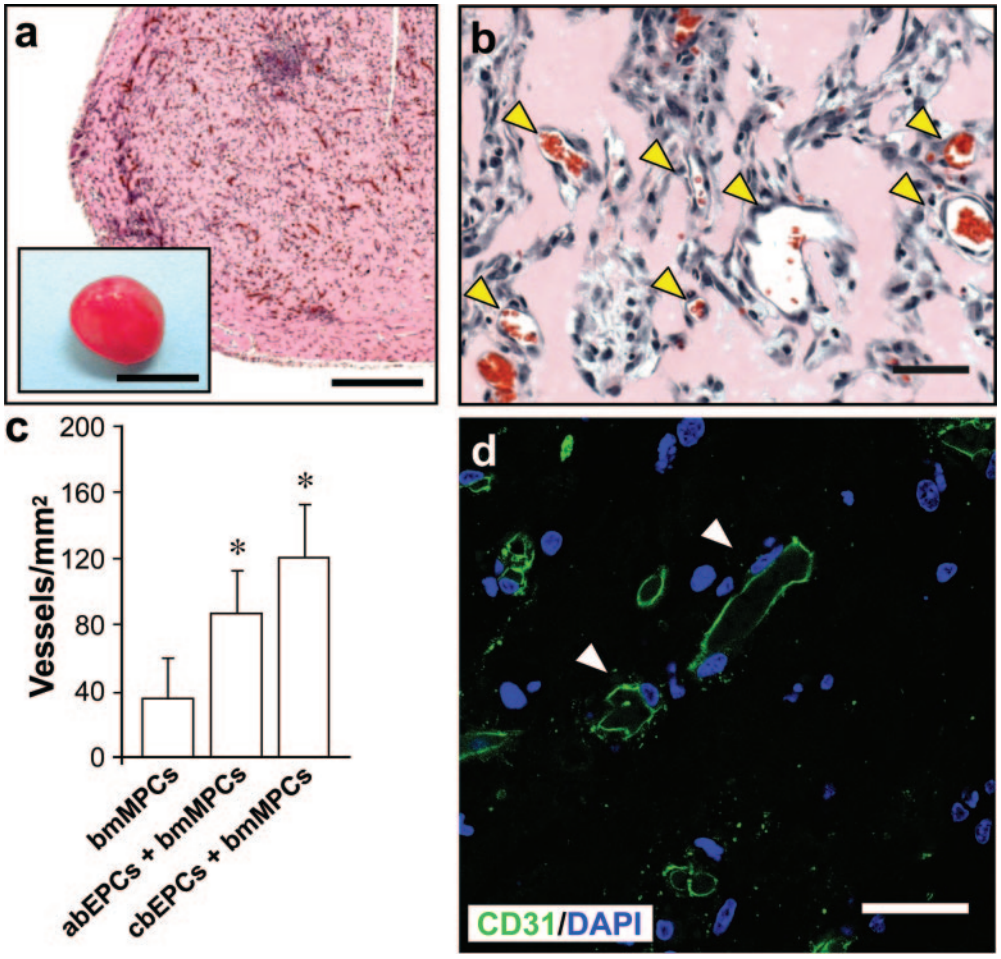

Figure 6. Vascular network formation using adult progenitor cells. Matrigel implants containing 40% abEPCs and 60% bmMPCs (obtained from human adult peripheral blood and adult bone marrow samples, respectively) were injected subcutaneously on the backs of 6-week-old nu/nu mice and evaluated after 1 week. a and b, H&E staining showed a uniform and extensive presence of lumenal structures containing erythrocytes (yellow arrowheads in b) throughout the implants. Scale bar in a, 500 μm; macroscopic view of explanted Matrigel plug is shown in the inset in a (scale bar=5 mm). Scale bar in b, 50 μm. c, Quantification of microvessel density was performed in implants seeded with bmMPCs in the absence or presence of either abEPCs or cbEPCs by counting erythrocyte-filled vessels. Each bar represents the mean microvessel density determined from 4 separate implants and mice±SD (vessels/mm^2). *$P<0.05$ compared with implants with bmMPCs alone (n=4). d, Microvessels from implants containing 40% abEPCs and 60% bmMPCs stained positive for human CD31 (white arrow heads), confirming that those lumens were formed by the implanted cells. Scale bar=30 μm. Images are representative of implants harvested from 4 different mice.

immunodeficient mice in the presence or absence of bmMPCs. At 1 and 4 weeks, mice were given the substrate luciferin by intraperitoneal injection (Figure 5f). No bioluminescence was detected in implants with luciferase-expressing cbEPCs alone, indicating that the substrate did not diffuse into the Matrigel. In contrast, a strong bioluminescent signal was detected in xenografts in which bmMPCs were coimplanted. This result, coupled with parallel histological data, confirmed that the presence of MPCs was crucial to achieve rapid perfusion of the implants. Importantly, the luciferase-dependent signal was still detected 4 weeks after implantation, a further indication of the long-lasting nature of the engineered vessels.

The cells within the Matrigel implants appeared to undergo a process of in vivo remodeling characterized by stabilization of total cellularity (supplemental Figure X) and progressive restriction of α-SMA–expressing cells to perivascular locations (Figure 5g through 5j), as expected in normal stabilized vasculature.[34] Finally, after 28 days in vivo, adipocytes were identified by staining with an anti-perilipin antibody (supplemental Figure XI), suggesting a process of integration between the implants and the surrounding murine adipose tissue.[35]

Vascular Network Formation Using Adult Progenitor Cells

We previously showed that adult peripheral blood–derived EPCs (abEPCs) combined with mature SMCs at a ratio of 4:1 (EPCs:SMCs) are vasculogenic in vivo, yet required higher seeding densities to achieve microvessel densities similar to that obtained with cbEPCs.[15] This apparently lower vasculogenic capacity of abEPCs has been suggested recently by others.[16] We hypothesized that the combination of adult bmMPCs and abEPCs at an "optimized ratio" (Figure 3k) would yield a high density vascular network. Indeed, there are no previous reports on adult human bmMPCs and abEPCs in the context of in vivo vasculogenesis. To evaluate this interaction, we isolated abEPCs as described[13–15] and confirmed their endothelial phenotype (supplemental Figure XII).

We implanted a total of 1.9×10^6 cells (40% abEPCs and 60% bmMPCs) in Matrigel by subcutaneous injection into immunodeficient mice (Figure 6). After harvesting the implants at 7 days (n=4), H&E staining consistently showed an extensive presence of blood vessels containing erythrocytes (Figure 6a and 6b). In addition, the lumenal structures stained positive for human CD31 (Figure 6d), confirming the lumens were formed by the implanted human abEPCs. Quantification of microvessel density (Figure 6c) revealed that the use of 40% abEPCs resulted in a statistically significant ($P<0.05$) increase in the number of blood vessels (86±26 vessels/mm^2) as compared with implants with bmMPCs alone (34±25 vessels/mm^2). Moreover, the difference between implants composed of abEPCs:bmMPCs and those of cbEPCs:

bmMPCs (119±33 vessels/mm^2) was not statistically significant (P=0.158), indicating that the presence of bmMPCs supported the vasculogenic properties of abEPCs to the same extent as was achieved with cbEPCs. These results show that a 2-cell system composed of human adult EPCs and MPCs exhibit the same robust in vivo vasculogenic activity as cbEPCs combined with adult bmMPCs, which is in contrast to conclusions drawn from experiments reported by others using a murine 10T1/2 cell line.[16]

Discussion

Here, we show that human postnatal EPCs and MPCs isolated from either blood or bone marrow have an inherent vasculogenic ability that can be exploited to create functional microvascular networks in vivo. Using Matrigel as a supporting scaffold,[15] we have shown that coimplantation of EPCs with either bmMPCs or cbMPCs into immunodeficient mice resulted in formation of extensive vascular networks after 1 week. The presence of human EPC-lined lumens containing erythrocytes (>100 vessels/mm^2) throughout the implants indicated not only a process of vasculogenesis from the 2 cell types but also the formation of functional anastomoses with the host circulatory system. In addition, MPCs were shown to reside in perivascular locations around the engineered lumens, confirming their active participation in blood vessel assembly. In vitro, MPCs were shown to differentiate into smMHC-positive cells when cocultured with EPCs, an indication that the MPCs achieved a mature smooth muscle phenotype. In a recent report, human mesenchymal stem cells combined with human umbilical vein ECs were shown to facilitate blood vessel assembly and adopt a perivascular location,[36] but our study differs from this report in that we show EPCs from either adult or cord blood, combined with MPCs from adult bone marrow or cord blood, form robust vascular networks in vivo. The extent of the engineered vascular networks was highly influenced by the ratio of EPCs to MPCs, with a progressive increase in vessel density and consistency of vascularized implants achieved when the contribution of MPCs was raised to 60% (Figure 3). This was true for both abEPCs and cbEPCs (Figure 6), demonstrating that both cord blood and adult peripheral blood are excellent sources of ECs for tissue vascularization.

Previous studies suggested the possibility of using mature ECs derived from vascular tissue to create microvascular networks.[7–9,37] However, the clinical use of mature ECs derived from autologous vascular tissue is limited by the difficulty of obtaining sufficient quantities of cells with minimal donor site morbidity.[1] Human ESCs have unlimited expansion capacity, but the therapeutic use of ESCs-derived ECs remains years away from the clinic. Most of these hurdles would be resolved if postnatal progenitor cells with expansion and functional potential were available from individual patients or from dedicated cell banks. In this regard, the in vitro expansion of blood-derived EPCs[12–15] and the recent confirmation of their ability to form vascular networks in vivo[15–17] have constituted major steps forward to resolve the problem of EC sourcing for therapeutic vasculogenesis.

Importantly, these studies have also shown that to produce high density and stable vascular networks, EPCs require coimplantation with perivascular cells. This is consistent with the literature showing interactions between ECs and perivascular cells in the blood vessel wall are critical for normal vascular development.[32–34] In previous attempts to create vascular networks with blood-derived EPCs, either mature SMCs[15] or the mouse embryonic cell line 10T1/2[16] were used to serve as perivascular cells; however, neither source is suitable for clinical application. Therefore, identification of MPCs as a readily obtainable perivascular cell source to partner in vivo with EPCs constitutes a crucial step in the development of therapeutic vasculogenesis. The numbers of human MPCs we were able to obtain in this study are likely to exceed, in the case of bone marrow, and be sufficient, in the case of cord blood, what would be needed for most autologous regenerative therapies.

This study has shown that successful in vivo vascularization depends on several distinct cellular functions. Firstly, both EPCs and MPCs must be present to initiate vasculogenesis, a process that was characterized by the formation of lumenal structures composed of human EPCs surrounded by α-SMA–positive mesenchymal cells. Secondly, an angiogenic response from the host vasculature is needed so that host vessels will be available to form anastomoses with the nascent vasculature. In this regard, we propose that the implanted MPCs stimulated the host angiogenic response. This is based on (1) the ability of bmMPCs alone to recruit murine vessels into the Matrigel implant and (2) the secretion of VEGF from MPCs in vitro (supplemental Figure VIII). EPCs did not secrete VEGF and did not stimulate murine vessel infiltration. Vascularization is achieved when the angiogenic and vasculogenic blood vessels meet, form anastomoses, and establish perfusion of the implants. The fact that perfusion occurred was supported by the presence of erythrocytes within the newly formed vasculature and the delivery of luciferin substrate from the peritoneal cavity to Matrigel implants containing both cbEPCs and bmMPCs. Subsequently, a process reminiscent of in vivo remodeling, characterized by a progressive restriction of α-SMA–expressing cells to perivascular locations, was seen, suggesting a stabilized vasculature.[34] Whether factors secreted or presented by MPCs contribute to such stabilization would be important to elucidate in a future study. Finally, our engineered vascular networks were patent for up to 4 weeks in vivo, confirming the capacity of EPC/MPC-derived vasculature to remain stable and functional.[16]

In summary, we have demonstrated the feasibility of engineering vascular networks in vivo with human postnatal progenitor cells that can be obtained by noninvasive procedures. In addition, we suggest that this murine model of human vasculogenesis is ideally suited for future studies on the cellular and molecular components of microvessel development and pathological neovascular responses and for the development of strategies to enhance neovascularization of engineered human tissues and organs. Further efforts are required to implement these vascularization strategies into tissue regeneration and tissue engineering applications.

Acknowledgments

We thank Dr Joseph C. Wu (Department of Radiology and Molecular Imaging Program, Stanford University School of Medicine,

Calif) for providing the pUb-fluc-GFP construct, Dr Masanori Aikawa (Brigham and Women's Hospital) for providing SMCs, Elke Pravda for confocal microscopy, Sandra R. Smith for VEGF analysis, Jill Wylie-Sears for technical assistance, and Kristin Johnson for figure preparation.

Sources of Funding

This work was supported by US Army Medical Research and Material Command (W81XWH-05-1-0115).

Disclosures

None.

References

1. Jain RK, Au P, Tam J, Duda DG, Fukumura D. Engineering vascularized tissue. *Nat Biotechnol*. 2005;23:821–823.
2. Isner JM, Asahara T. Angiogenesis and vasculogenesis as therapeutic strategies for postnatal neovascularization. *J Clin Invest*. 1999;103:1231–1236.
3. Isner JM, Pieczek A, Schainfeld R, Blair R, Haley L, Asahara T, Rosenfield K, Razvi S, Walsh K, Symes JF. Clinical evidence of angiogenesis after arterial gene transfer of phVEGF165 in patient with ischaemic limb. *Lancet*. 1996;348:370–374.
4. Lee H, Cusick RA, Browne F, Ho Kim T, Ma PX, Utsunomiya H, Langer R, Vacanti JP. Local delivery of basic fibroblast growth factor increases both angiogenesis and engraftment of hepatocytes in tissue-engineered polymer devices. *Transplantation*. 2002;73:1589–1593.
5. Li X, Tjwa M, Moons L, Fons P, Noel A, Ny A, Zhou JM, Lennartsson J, Li H, Luttun A, Ponten A, Devy L, Bouche A, Oh H, Manderveld A, Blacher S, Communi D, Savi P, Bono F, Dewerchin M, Foidart JM, Autiero M, Herbert JM, Collen D, Heldin CH, Eriksson U, Carmeliet P. Revascularization of ischemic tissues by PDGF-CC via effects on endothelial cells and their progenitors. *J Clin Invest*. 2005;115:118–127.
6. Rafii S, Lyden D. Therapeutic stem and progenitor cell transplantation for organ vascularization and regeneration. *Nat Med*. 2003;9:702–712.
7. Koike N, Fukumura D, Gralla O, Au P, Schechner JS, Jain RK. Tissue engineering: creation of long-lasting blood vessels. *Nature*. 2004;428:138–139.
8. Nor JE, Peters MC, Christensen JB, Sutorik MM, Linn S, Khan MK, Addison CL, Mooney DJ, Polverini PJ. Engineering and characterization of functional human microvessels in immunodeficient mice. *Lab Invest*. 2001;81:453–463.
9. Schechner JS, Nath AK, Zheng L, Kluger MS, Hughes CC, Sierra-Honigmann MR, Lorber MI, Tellides G, Kashgarian M, Bothwell AL, Pober JS. In vivo formation of complex microvessels lined by human endothelial cells in an immunodeficient mouse. *Proc Natl Acad Sci U S A*. 2000;97:9191–9196.
10. Levenberg S, Rouwkema J, Macdonald M, Garfein ES, Kohane DS, Darland DC, Marini R, van Blitterswijk CA, Mulligan RC, D'Amore PA, Langer R. Engineering vascularized skeletal muscle tissue. *Nat Biotechnol*. 2005;23:879–884.
11. Wang ZZ, Au P, Chen T, Shao Y, Daheron LM, Bai H, Arzigian M, Fukumura D, Jain RK, Scadden DT. Endothelial cells derived from human embryonic stem cells form durable blood vessels in vivo. *Nat Biotechnol*. 2007;25:317–318.
12. Asahara T, Murohara T, Sullivan A, Silver M, van der Zee R, Li T, Witzenbichler B, Schatteman G, Isner JM. Isolation of putative progenitor endothelial cells for angiogenesis. *Science*. 1997;275:964–967.
13. Ingram DA, Mead LE, Tanaka H, Meade V, Fenoglio A, Mortell K, Pollok K, Ferkowicz MJ, Gilley D, Yoder MC. Identification of a novel hierarchy of endothelial progenitor cells using human peripheral and umbilical cord blood. *Blood*. 2004;104:2752–2760.
14. Lin Y, Weisdorf DJ, Solovey A, Hebbel RP. Origins of circulating endothelial cells and endothelial outgrowth from blood. *J Clin Invest*. 2000;105:71–77.
15. Melero-Martin JM, Khan ZA, Picard A, Wu X, Paruchuri S, Bischoff J. In vivo vasculogenic potential of human blood-derived endothelial progenitor cells. *Blood*. 2007;109:4761–4768.
16. Au P, Daheron LM, Duda DG, Cohen KS, Tyrrell JA, Lanning RM, Fukumura D, Scadden DT, Jain RK. Differential in vivo potential of endothelial progenitor cells from human umbilical cord blood and adult peripheral blood to form functional long-lasting vessels. *Blood*. 2008;111:1302–1305.
17. Yoder MC, Mead LE, Prater D, Krier TR, Mroueh KN, Li F, Krasich R, Temm CJ, Prchal JT, Ingram DA. Redefining endothelial progenitor cells via clonal analysis and hematopoietic stem/progenitor cell principals. *Blood*. 2007;109:1801–1809.
18. Pittenger MF, Mackay AM, Beck SC, Jaiswal RK, Douglas R, Mosca JD, Moorman MA, Simonetti DW, Craig S, Marshak DR. Multilineage potential of adult human mesenchymal stem cells. *Science*. 1999;284:143–147.
19. Simper D, Stalboerger PG, Panetta CJ, Wang S, Caplice NM. Smooth muscle progenitor cells in human blood. *Circulation*. 2002;106:1199–1204.
20. Kim JW, Kim SY, Park SY, Kim YM, Kim JM, Lee MH, Ryu HM. Mesenchymal progenitor cells in the human umbilical cord. *Ann Hematol*. 2004;83:733–738.
21. Le Ricousse-Roussanne S, Barateau V, Contreres JO, Boval B, Kraus-Berthier L, Tobelem G. Ex vivo differentiated endothelial and smooth muscle cells from human cord blood progenitors home to the angiogenic tumor vasculature. *Cardiovasc Res*. 2004;62:176–184.
22. Lee OK, Kuo TK, Chen WM, Lee KD, Hsieh SL, Chen TH. Isolation of multipotent mesenchymal stem cells from umbilical cord blood. *Blood*. 2004;103:1669–1675.
23. Traktuev D, Merfeld-Clauss S, Li J, Kolonin M, Arap W, Pasqualini R, Johnstone BH, March KL. A population of multipotent CD34-positive adipose stromal cells share pericyte and mesenchymal surface markers, reside in a periendothelial location, and stabilize endothelial networks. *Circ Res*. 2008;102:77–85.
24. Marion NW, Mao JJ. Mesenchymal stem cells and tissue engineering. *Methods Enzymol*. 2006;420:339–361.
25. Madsen CS, Regan CP, Hungerford JE, White SL, Manabe I, Owens GK. Smooth muscle-specific expression of the smooth muscle myosin heavy chain gene in transgenic mice requires 5′-flanking and first intronic DNA sequence. *Circ Res*. 1998;82:908–917.
26. Miano JM, Cserjesi P, Ligon KL, Periasamy M, Olson EN. Smooth muscle myosin heavy chain exclusively marks the smooth muscle lineage during mouse embryogenesis. *Circ Res*. 1994;75:803–812.
27. Digirolamo CM, Stokes D, Colter D, Phinney DG, Class R, Prockop DJ. Propagation and senescence of human marrow stromal cells in culture: a simple colony-forming assay identifies samples with the greatest potential to propagate and differentiate. *Br J Haematol*. 1999;107:275–281.
28. Wall ME, Bernacki SH, Loboa EG. Effects of serial passaging on the adipogenic and osteogenic differentiation potential of adipose-derived human mesenchymal stem cells. *Tissue Eng*. 2007;13:1291–1298.
29. Antonelli-Orlidge A, Saunders KB, Smith SR, D'Amore PA. An activated form of transforming growth factor beta is produced by cocultures of endothelial cells and pericytes. *Proc Natl Acad Sci U S A*. 1989;86:4544–4548.
30. Hirschi KK, Rohovsky SA, D'Amore PA. PDGF, TGF-beta, and heterotypic cell-cell interactions mediate endothelial cell-induced recruitment of 10T1/2 cells and their differentiation to a smooth muscle fate. *J Cell Biol*. 1998;141:805–814.
31. Wu X, Rabkin-Aikawa E, Guleserian KJ, Perry TE, Masuda Y, Sutherland FW, Schoen FJ, Mayer JE Jr, Bischoff J. Tissue-engineered microvessels on three-dimensional biodegradable scaffolds using human endothelial progenitor cells. *Am J Physiol Heart Circ Physiol*. 2004;287:H480–H487.
32. Darland DC, D'Amore PA. Blood vessel maturation: vascular development comes of age. *J Clin Invest*. 1999;103:157–158.
33. Folkman J, D'Amore PA. Blood vessel formation: what is its molecular basis? *Cell*. 1996;87:1153–1155.
34. Jain RK. Molecular regulation of vessel maturation. *Nat Med*. 2003;9:685–693.
35. Fukumura D, Ushiyama A, Duda DG, Xu L, Tam J, Krishna V, Chatterjee K, Garkavtsev I, Jain RK. Paracrine regulation of angiogenesis and adipocyte differentiation during in vivo adipogenesis. *Circ Res*. 2003;93:e88–e97.
36. Au P, Tam J, Fukumura D, Jain RK. Bone marrow derived mesenchymal stem cells facilitate engineering of long-lasting functional vasculature. *Blood*. 2008;111:4551–4558.
37. Shepherd BR, Chen HY, Smith CM, Gruionu G, Williams SK, Hoying JB. Rapid perfusion and network remodeling in a microvascular construct after implantation. *Arterioscler Thromb Vasc Biol*. 2004;24:898–904.

EXPANDED MATERIALS AND METHODS and SUPPLEMENTAL FIGURES

Isolation and culture of EPCs

Human umbilical cord blood was obtained from the Brigham and Women's Hospital in accordance with an Institutional Review Board-approved protocol. Adult peripheral blood was collected from volunteer donors in accordance with a protocol approved by Children's Hospital Boston Committee on Clinical Investigation. EPCs were isolated from the mononuclear cell (MNC) fractions of both cord blood (cbEPCs; n=19) and adult peripheral blood (abEPCs; n=3) samples, and purified using CD31-coated magnetic beads [1]. EPCs were subcultured on fibronectin-coated (FN; 1 μg/cm^2; Chemicon International, Temecula, CA) plates using EPC-medium: EGM-2 (except for hydrocortisone; Lonza, Walkersville, MD) supplemented with 20% FBS (Hyclone, Logan, UT), 1x glutamine-penicillin-streptomycin (GPS; Invitrogen, Carlsbad, CA). EPCs between passages 5 and 7 were used for all experiments.

Isolation and culture of MPCs

bmMPCs were isolated from the MNC fraction of a 25 mL human bone marrow sample (Cambrex Bio Science, Walkersville, MD). MNCs were seeded on 1% gelatin-coated tissue culture plates using EGM-2 (except for hydrocortisone, VEGF, bFGF, and heparin), 20% FBS, 1x GPS and 15% autologous plasma. Unbound cells were removed at 48 hours, and the bound cell fraction maintained in culture until 70% confluence using MPC-medium: EGM-2 (except for hydrocortisone, VEGF, bFGF, and heparin), 20% FBS, and 1x GPS. Commercially available bmMPCs (Cambrex) were used as control to those isolated in our laboratory. Similarly, cbMPCs were isolated from the MNC

fractions of 25 mL human cord blood samples (n=5). Unbound cells were removed at 48 hours, and the bound cell fraction maintained in culture using MPC-medium. cbMPCs emerged in culture forming mesenchymal-like colonies after one week. These cbMPCs colonies were selected with cloning rings and cultured separately from the rest of the adherent cells. Thereafter, both bmMPCs and cbMPCs were subcultured on FN-coated plates using MPC-medium. MPCs between passages 4 and 9 were used for all the experiments.

Cell expansion potential

cbEPCs and MPCs were isolated from 25 mL of either cord blood or bone marrow and serially expanded in culture using EPC-medium and MPC-medium respectively. All passages were performed by plating the cells onto 1 μg/cm^2 FN-coated tissue culture plates at either 5x10^3 cell/cm^2 (cbEPCs) or 1x10^4 cell/cm^2 (MPCs). Medium was refreshed every 2-3 days and cells were harvested by trypsinization and re-plated using the same culture conditions for each passage. Cumulative values of total cell number were calculated after 25, 40 and 60 days in culture by counting the cells at the end of each passage using a haemocytometer.

Flow cytometry

Cytometric analyses were carried out by labeling with phycoerythrin (PE)-conjugated mouse anti-human CD31 (Ancell, Bayport, MN), PE- conjugated mouse anti-human CD90 (Chemicon International), PE-conjugated mouse anti-human CD105 (1:50; Serotec, Raleigh, NC), PE-conjugated mouse anti-human CD44 (1:100; BD

PharMingen), PE-conjugated mouse anti-human CD34 (1:50; Miltenyi Biotec, Auburn, CA), PE-conjugated mouse anti-human VEGF-R2 (1:50; R&D Systems, Minneapolis, MN), PE-conjugated mouse anti-human Neuropilin-1 (1:100; Miltenyi Biotec), fluorescein isothiocyanate (FITC)-conjugated mouse anti-human CD45 (BD PharMingen, San Jose, CA), FITC-conjugated mouse anti-human CD29 (1:100; Immunotech/Beckman Coulter, Fullerton, CA), FITC-conjugated mouse anti-human CD146 (1:100; Chemicon International), FITC-conjugated mouse anti-human CD14 (1:100; BD PharMingen), FITC-mouse IgG_1 (BD PharMingen), and PE-mouse IgG_1 (BD PharMingen) antibodies (1:100). Antibody labeling was carried out for 20 minutes on ice followed by 3 washes with PBS/1% BSA/0.2 mM EDTA and resuspension in 1% paraformaldehyde in PBS. Flow cytometric analyses were performed using a Becton Dickinson FACScan flow cytometer and FlowJo software (Tree Star Inc., Ashland, OR). Human dermal microvascular ECs (HDMECs) from newborn foreskin, SMCs from human saphenous vein, and adult peripheral blood monocytes (pbMonocytes) served as controls.

Western blot

Cells were lysed with 4 mol/L urea, 0.5% SDS, 0.5% NP-40, 100 mmol/L Tris, and 5 mmol/L EDTA, pH 7.4, containing a protease inhibitor cocktail Complete Mini tablet (Roche Diagnostics, Indianapolis, IN). Lysates were subjected to 10% SDS-PAGE (10 μg of protein per lane) and transferred to Immobilon-P membrane. Membranes were incubated with respective primary antibodies, goat anti-human CD31 (1:500; Santa Cruz Biotechnology, Santa Cruz, CA), goat anti-human VE-cadherin (1:10,000; Santa Cruz

Biotechnology), mouse anti-human α-SMA (1:2000; Sigma-Aldrich, St. Louis, MO), mouse anti-human calponin (1:500; Sigma-Aldrich), and mouse anti-human β-actin (1:10,000; Sigma-Aldrich) diluted in 1x PBS, 5% dry milk, 0.1% Tween-20, and then with secondary antibodies (1:5000; peroxidase-conjugated anti-goat or anti-mouse; Vector Laboratories, Burlingame, CA). Antigen-antibody complexes were visualized using Lumiglo and chemiluminescent sensitive film. SMCs isolated from human saphenous veins and grown in DMEM, 10% FBS, 1x GPS, and 1x non-essential amino acids served as control.

Western blot analysis of PDGF-Rβ

MPCs were plated at a density of $1x10^4$ cell/cm^2 onto FN-coated plates and cultured using DMEM, 10% FBS, and 1X GPS in the presence or absence of TGF-β1 (2 ng/ml), PDGF-BB (50 ng/ml), and a combination of TGF-β1 + PDGF-BB (2 ng/ml + 50 ng/ml). Cell lysates were harvested after 6 days and Western blot analysis carried out using goat anti-human PDGF-Rβ (1:250; Santa Cruz Biotechnology), mouse anti-human β-actin (1:10000; Sigma-Aldrich) and peroxidase-conjugated anti-goat or anti- mouse secondary antibodies (1:5000; Vector Laboratories). SMCs served as control. Quantification was performed by image analysis of the bands (ImageJ software; NIH, Bethesda, MD).

Indirect immunofluorescence

Immunofluorescence was carried out using goat anti-human CD31 (1:200; Santa Cruz Biotechnology), mouse anti-human vWF (1:200; DakoCytomation), goat anti-human VE-

cadherin (1:200; Santa Cruz Biotechnology), mouse anti-human α-smooth muscle actin (1:2000; α-SMA; Sigma-Aldrich), mouse anti-human Calponin (1:100; DakoCytomation), mouse anti-human smooth muscle myosin heavy chain (1:100; Sigma-Aldrich), and mouse anti-human NG_2 (1:100; Sigma-Aldrich) antibodies, followed by FITC-conjugated secondary antibodies (1:200; Vector Laboratories) and Vectashield mounting medium with DAPI (Vector Laboratories).

Measurement of VEGF in cell supernatant

cbEPCs and MPCs were plated at a density of $2x10^4$ cell/cm^2 onto FN-coated 24-well plates using EPC- or MPC-medium respectively. After 24 hours, cells were washed and media replaced with DMEM containing 10% FBS, and 1X GPS and cell culture supernatant collected after 24 hours. Quantitative measurement of human VEGF in the cell culture supernatant was carried out using a Quantikine ELISA kit (R&D Systems, Minneapolis, MN). Values were normalized to total cell number determined at the time of supernatant collection.

Osteogenesis assay

Confluent MPCs were cultured for 10 days in DMEM low-glucose medium with 10% FBS, 1X GPS, and osteogenic supplements (1 μM dexamethasone, 10 mM β-glycerophosphate, 60 μM ascorbic acid-2-phosphate). Differentiation into osteocytes was assessed by alkaline phosphatase staining [2].

Chondrogenesis assay

Suspensions of MPCs were transferred into 15 ml polypropylene centrifuge tubes (500,000 cells/tube) and gently centrifuged. The resulting pellets were statically cultured in DMEM high-glucose medium with 1X GPS, and chondrogenic supplements (1X insulin-transferrin-selenium, 1 µM dexamethasone, 100 µM ascorbic acid-2-phosphate, and 10 ng/mL TGF-β1). After 14 days, pellets were fixed in 10% buffered formalin overnight, embedded in paraffin, and sectioned (7 µm-thick). Differentiation into chondrocytes was assessed by evaluating the presence of glycosaminoglycans after Alcian Blue staining. Sections of mouse articular cartilage served as control.

Adipogenesis assay

Confluent MPCs were cultured for 10 days in DMEM low-glucose medium with 10% FBS, 1X GPS, and adipogenic supplements (5 µg/mL insulin, 1 µM dexamethasone, 0.5 mM isobutylmethylxanthine, 60 µM indomethacin). Differentiation into adipocytes was assessed by Oil Red O staining [2].

Smooth muscle differentiation assay

cbEPCs were co-cultured with either bmMPCs or cbMPCs (1:1 EPCs to MPCs ratio) at a density of $2x10^4$ cell/cm^2 on FN-coated plates using EPC-medium. After 7 days, immunofluorescence was carried out using rabbit anti-human vWF (1:200; DakoCytomation, Carpinteria, CA), and mouse anti-human smooth muscle myosin heavy chain (1:100; Sigma-Aldrich) antibodies, followed by anti-rabbit TexasRed-conjugated, and anti-mouse FITC-conjugated secondary antibodies (1:200; Vector Laboratories). Vectashield with 4,6-diamidino-2-phenylindole (DAPI; Vector

Laboratories) was used as mounting medium. Monocultures of MPCs in EPC-medium served as control.

Indirect co-culture of cbEPCs and MPCs

cbEPCs were co-cultured with either bmMPCs or cbMPCs using a 0.4 µm Transwell-24 membrane culture system (Corning Incorporated Life Sciences, Acton, MA). cbEPCs were pre-cultured for 24 hours in the Transwell inserts at a density of $1x10^4$ cell/cm^2 after FN-coating using EPC-medium. Simultaneously, MPCs were pre-cultured separately onto FN-coated 24-wells at a density of $1x10^4$ cell/cm^2 using MPC-medium. After 24 hours, the top chambers where placed into the MPC wells and the resulting Transwell system cultured for 7 days using EPC-medium. Immunofluorescence was carried out using rabbit anti-human vWF (1:200; DakoCytomation), and mouse anti-human smooth muscle myosin heavy chain (1:100; Sigma-Aldrich) antibodies, followed by anti-rabbit TexasRed-conjugated, and anti-mouse FITC-conjugated secondary antibodies (1:200; Vector Laboratories). Vectashield with DAPI (Vector Laboratories) was used as mounting medium. SMCs served as control.

Retroviral transduction of cbEPCs and bmMPCs

GFP-labeled cells were generated by retroviral infection with a pMX-GFP vector using a modified protocol from Kitamura *et al.* [3]. Briefly, retroviral supernatant from HEK 293T cells was harvested and both cbEPC and bmMPCs ($1x10^6$ cells) were then incubated with 5 mL of virus stock for 6 hr in the presence of 8 µg/mL polybrene. GFP-expressing

cells were sorted by FACS, expanded under routine conditions, and used for *in vivo* vasculogenic assays.

In vivo vasculogenesis assay

The formation of vascular networks *in vivo* was evaluated using a xenograft model as described [1]. Briefly, a total of $1.9x10^6$ cells was resuspended in 200 µl of ice-cold Phenol Red-free Matrigel™ (BD Bioscience, San Jose, CA), at ratios of 100:0, 80:20, 60:40, 40:60, 20:80 and 0:100 (EPCs:MPCs). The mixture was implanted on the back of a six-week-old male athymic nu/nu mouse (Massachusetts General Hospital, Boston, MA) by subcutaneous injection using a 25-gauge needle. Implants of Matrigel alone served as controls. One implant was injected per mouse. Each experimental condition was performed with 4 mice.

Histology and immunohistochemistry

Mice were euthanized at different time points and Matrigel implants were removed, fixed in 10% buffered formalin overnight, embedded in paraffin, and sectioned. H&E stained 7 µm-thick sections were examined for the presence of lumenal structures containing red blood cells. For immunohistochemistry, 7-µm-thick sections were deparaffinized, and antigen retrieval was carried out by heating the sections in Tris-EDTA buffer (10mM Tris-Base, 2 mM EDTA, 0.05% Tween-20, pH 9.0). The sections were blocked for 30 minutes in 5-10% blocking serum and incubated with primary antibodies for 1 hour at room temperature. The following primary antibodies were used: mouse anti-human CD31 (for human microvessel detection; 1:20; DakoCytomation, M0823 Clone JC70A;

blocking with horse serum), goat anti-human CD31 (for CD31 and α-SMA co-staining; 1:20; Santa Cruz Biotechnology; blocking with rabbit serum), mouse anti-human α-SMA (1:750; Sigma-Aldrich; blocking with horse serum), rabbit anti-GFP antibody (1:4000; Abcam; blocking with goat serum), rabbit anti-human perilipin-A (1:750; Sigma-Aldrich), and mouse IgG (1:50; DakoCytomation; blocking with horse serum). Secondary antibody incubations were carried out for 1 hour at room temperature using either FITC- or TexasRed-conjugated antibodies (1:200; Vector Laboratories). For CD31 detection, biotinylated IgG /streptavidin-FITC conjugate (1:200; Vector Laboratories) incubations were carried out after primary antibodies. When double staining was performed, the sections were washed and blocked for 30 additional minutes in between the first secondary antibody and the second primary antibody. All the fluorescent-stained sections were counterstained with DAPI (Vector Laboratories). Projections of whole-mount GFP staining were performed on 100-µm-thick sections by confocal microscopy (71 sections over 50 µm). Additionally, horseradish peroxidase-conjugated mouse secondary antibody (1:200; Vector Laboratories) and 3,3'-diaminobenzidine (DAB) were used for detection of α-SMA, followed by hematoxilin counterstaining and Permount mounting. Human infantile hemangioma, and mouse skin and lung served as control tissues.

Microvessel density analysis

Microvessels were quantified by evaluation of 10 randomly selected fields (0.1 mm^2 each) of H&E stained sections taken from the middle part of the implants as described [1]. Microvessels were identified as lumenal structures containing red blood cells and

counted. Microvessels density was reported as the average number of red blood cell-filled microvessels from the fields analyzed and expressed as vessels/mm^2. Values reported for each experimental condition correspond to the average values ± S.D. obtained from at least four individual mice.

Luciferase assay

cbEPCs were infected with Lenti-pUb-fluc-GFP at a multiplicity of infection (MOI) of 10. The pUb-fluc-GFP was made based on the backbone of pHR-s1-cla. The CMV promoter was replaced by the ubiquitin promoter, followed by a firefly luciferase/GFP fusion gene [4]. Lentivirus was prepared by transient transfection of 293T cells. Briefly, pUb-fluc-GFP was cotransfected into 293T cells with HIV-1 packaging vector and vesicular stomatitis virus G glycoprotein-pseudotyped envelop vector (pVSVG). Collected supernatant was filtered using a syringe filter (0.45 µm) and concentrated by centrifuging at 5000g for 2 hours. The virus was titrated on 293T cells. The infectivity was determined by GFP expression and luciferase/GFP-expressing cbEPCs were further sorted by FACS, expanded under routine conditions, and used for *in vivo* vasculogenic assays. Luciferase/GFP-expressing cbEPCs were resuspended in 200 µl of Matrigel in the presence (40% cbEPC:60% bmMPCs) or absence of bmMPCs, at a total of 1.9x10^6 cells. The mixture was implanted on the back of a six-week-old male nu/nu mouse by subcutaneous injection. One implant was injected per mouse. Each experimental condition was performed with 4 mice. At various intervals after implantation, the mice were imaged using an IVIS 200 Imaging System (Xenogen Corporation, Alameda, CA). Mice were anesthetized using an isofluorane chamber and

were given the substrate, luciferin (2.5 mg/mL), by intraperitoneal injection according to their weights (typically 250 µl/30 gr). Bioluminescence was detected in implants 30-40 min after luciferin administration, and the collected data analyzed with Live Image 3.0 (Xenogen Corporation).

Cellularity of Matrigel implants

Mice were euthanized at different time points and Matrigel implants were removed, fixed in 10% buffered formalin overnight, embedded in paraffin, and sectioned. 7-µm-thick sections were deparaffinized and mounted with Vectashield with DAPI (Vector Laboratories). Cell nuclei were visualized using a fluorescent microscope, and counted in 4 randomly selected fields (0.29 mm^2 each) of sections taken from the middle part of the implants. Cellularity was reported as the average number of nuclei from the fields analyzed and expressed as cells/mm^2. Values reported for each experimental condition correspond to the average values ± S.D. obtained from at four individual mice.

Microscopy

Phase microscopy images were taken with a Nikon Eclipse TE300 inverted microscope (Nikon, Melville, NY) using Spot Advance 3.5.9 software (Diagnostic Instruments, Sterling Heights, MI) and 10x/0.3 objective lens. All fluorescent images were taken with a Leica TCS SP2 Acousto-Optical Beam Splitter confocal system equipped with DMIRE2 inverted microscope (Diode 405 nm, Argon 488 nm, HeNe 594 nm; Leica Microsystems, Wetzlar, Germany) using either 20x/0.7 imm, 63x/1.4 oil, or 100x/1.4 oil objective lens. Non-fluorescent images were taken with a Axiophot II fluorescence

microscope (Zeiss, Oberkochen, Germany) equipped with AxioCam MRc5 camera (Zeiss) using either 2.5x/0.075 or 40x/1.0 oil objective lens.

Statistical analysis

The data were expressed as means ± SD. Where appropriate, analysis of variance (ANOVA) followed by two-tailed Student's unpaired t-tests were performed. *P* value < 0.05 was considered a statistically significant difference.

References

1. Melero-Martin JM, Khan ZA, Picard A, Wu X, Paruchuri S, Bischoff J. In vivo vasculogenic potential of human blood-derived endothelial progenitor cells. *Blood.* 2007;109:4761-4768.

2. Pittenger MF, Mackay AM, Beck SC, Jaiswal RK, Douglas R, Mosca JD, Moorman MA, Simonetti DW, Craig S, Marshak DR. Multilineage potential of adult human mesenchymal stem cells. *Science.* 1999;284:143-147.

3. Kitamura T, Onishi M, Kinoshita S, Shibuya A, Miyajima A, Nolan GP. Efficient screening of retroviral cDNA expression libraries. *Proc Natl Acad Sci U S A.* 1995;92:9146-9150.

4. Wu JC, Cao F, Dutta S, Xie X, Kim E, Chungfat N, Gambhir S, Mathewson S, Connolly AJ, Brown M, Wang EW. Proteomic analysis of reporter genes for molecular imaging of transplanted embryonic stem cells. *Proteomics.* 2006;6:6234-6249.

Supplementary Table 1. Effect of EPC:MPC ratio on *in vivo* vascularization

	cbEPC:MPC Ratio					
	100:0	80:20	60:40	40:60	20:80	0:100
Source of MPCs	Number of vascularized/total implants					
bmMPCs	0/8	7/8	3/4	4/4	4/4	4/4
cbMPCs	0/8	3/6	2/4	4/4	4/4	2/4

Supplementary Figure 1. Morphology of EPCs and MPCs

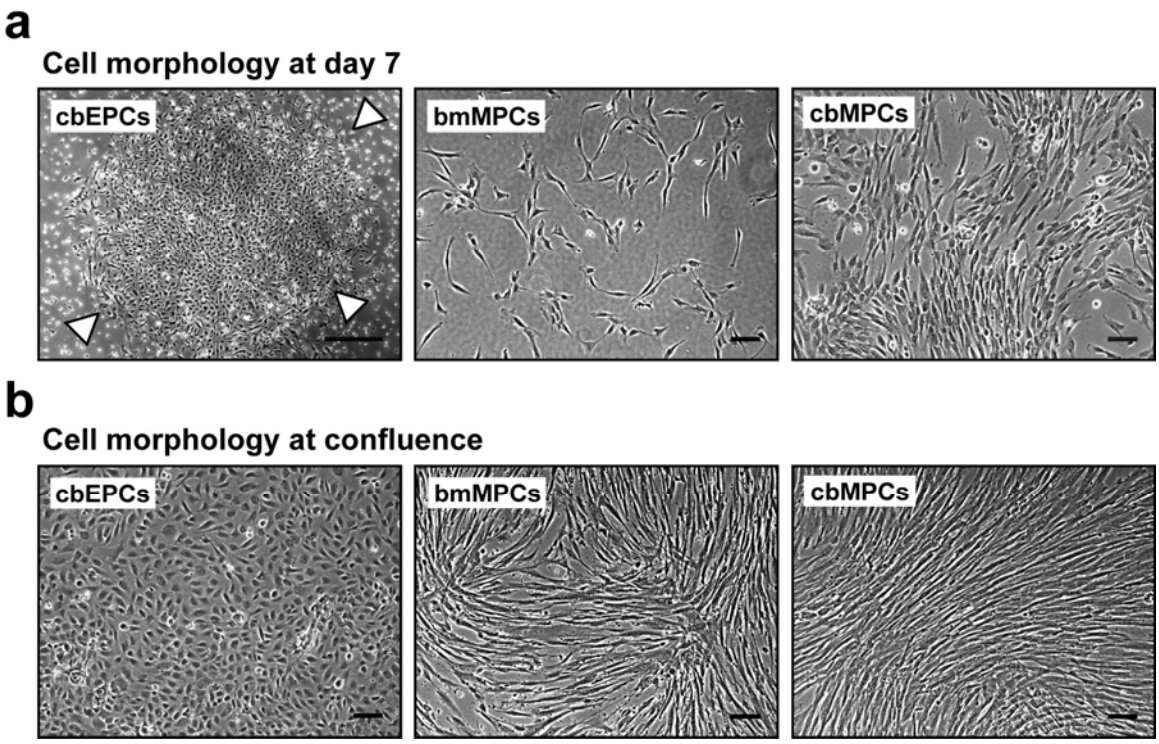

(a) During the first week of isolation, cbEPCs emerged forming typical EC colonies, bmMPCs adhered uniformly to the culture plates and cbMPCs emerged forming mesenchymal-like colonies. (b) At confluence, cbEPCs presented typical cobblestone morphology, while both bmMPCs and cbMPCs presented spindle morphology characteristic of mesenchymal cells in culture (scale bar of cbEPCs colony, 500 µm; rest of scale bars, 100 µm).

Supplementary Figure 2. Flow cytometric characterization of EPCs and MPCs

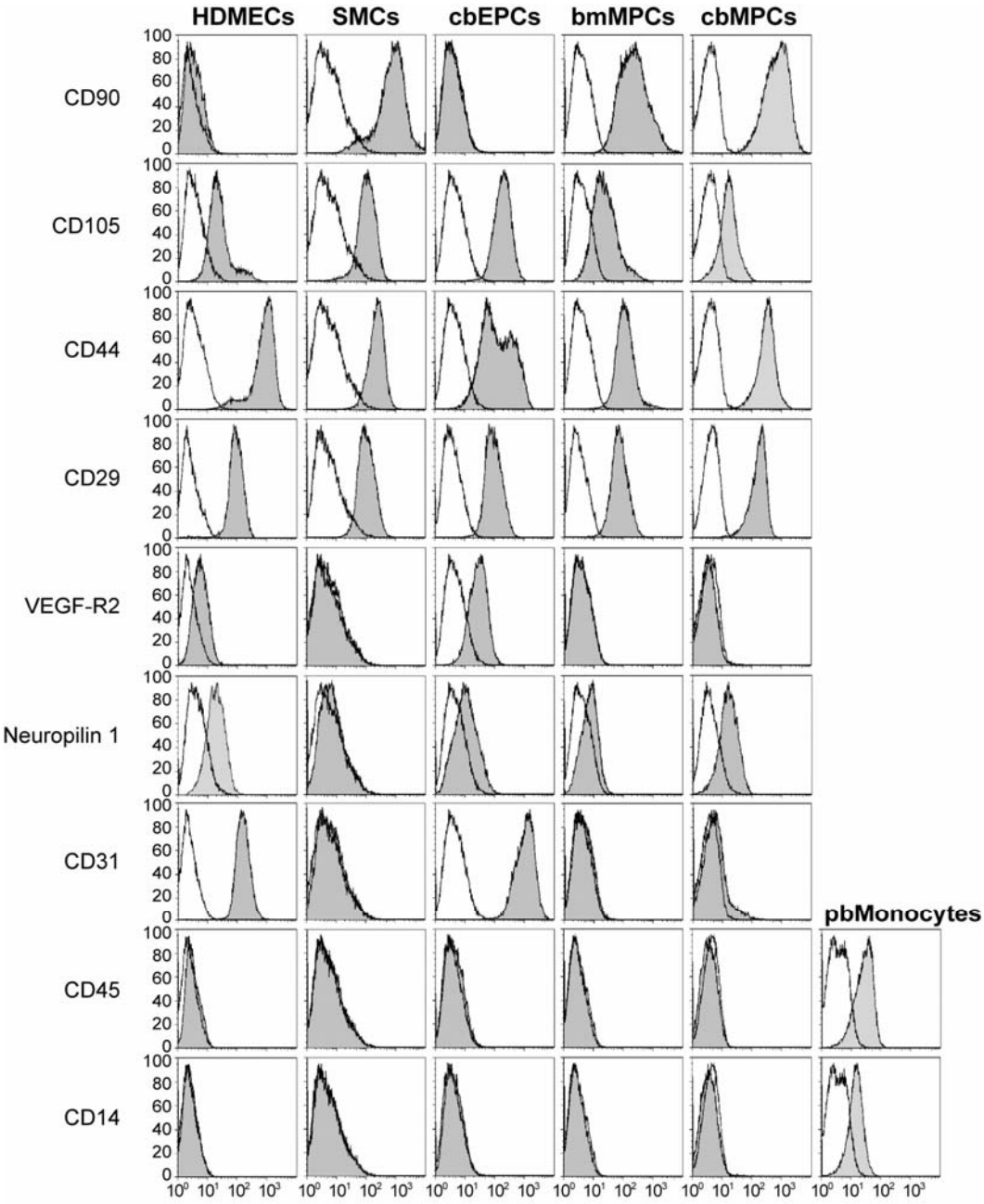

Cytometric analyses were carried out by labeling with either PE- or FITC-conjugated antibodies. Flow cytometric analyses were performed using a Becton Dickinson FACScan flow cytometer and FlowJo software. Solid gray histograms represent cells stained with fluorescent antibodies. Isotype-matched controls are overlaid in a black line on each histogram. HDMECs, SMCs, and peripheral blood monocytes (pbMonocytes) served as control for EC, mesenchymal, and hematopoietic cells respectively.

Supplementary Figure 3. Immunofluorescence characterization of EPCs and MPCs

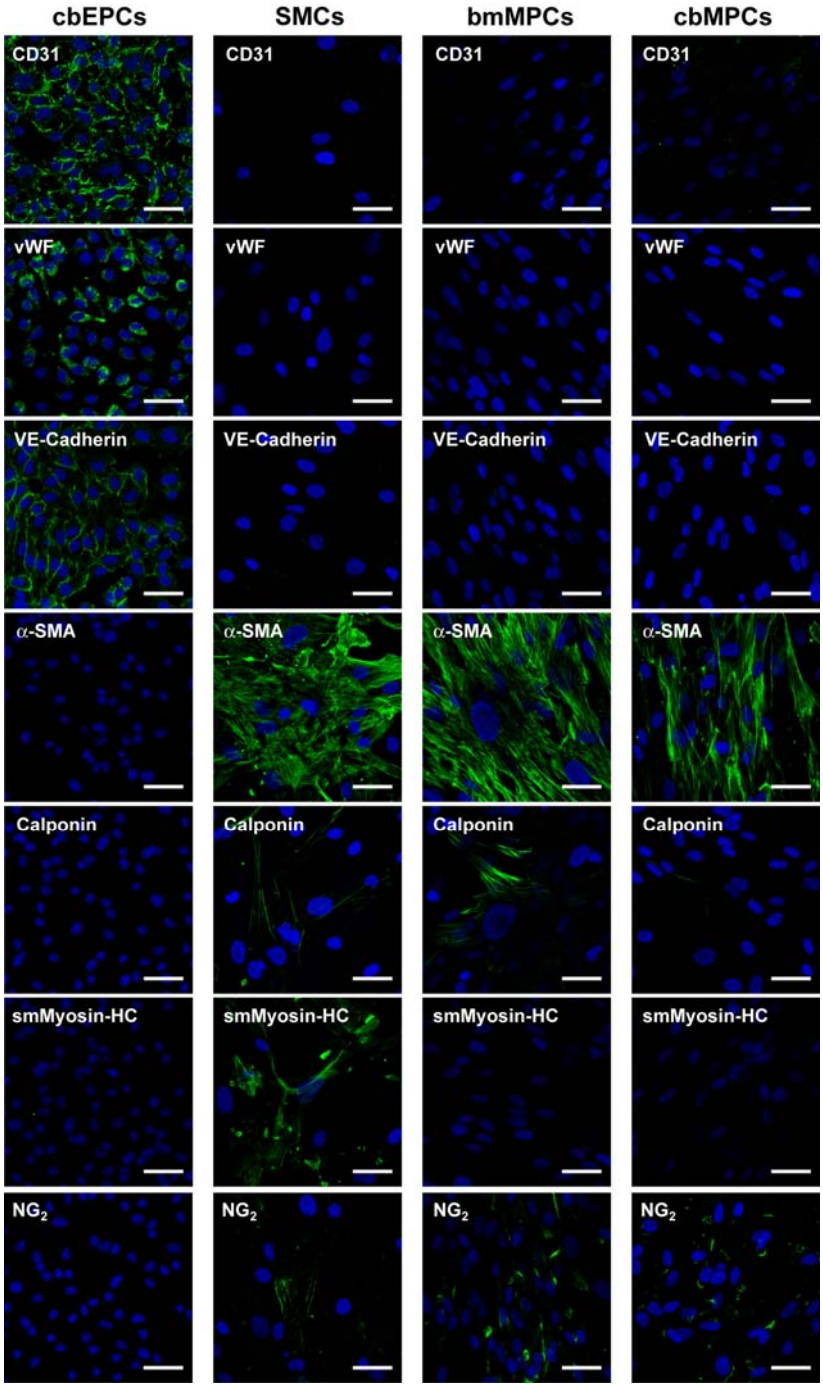

cbEPCs expressed endothelial markers CD31, VE-Cadherin and vWF as determined by indirect immunofluorescence. Both bmMPCs and cbMPCs expressed mesenchymal markers α-SMA, calponin, and NG_2, but not the smooth muscle marker smMyosin-HC. SMCs obtained from human sapheneous vein served as control (scale bars, 50 µm).

Supplementary Figure 4. Differentiation of MPCs into adipocytes, osteocytes, and Chondrocytes

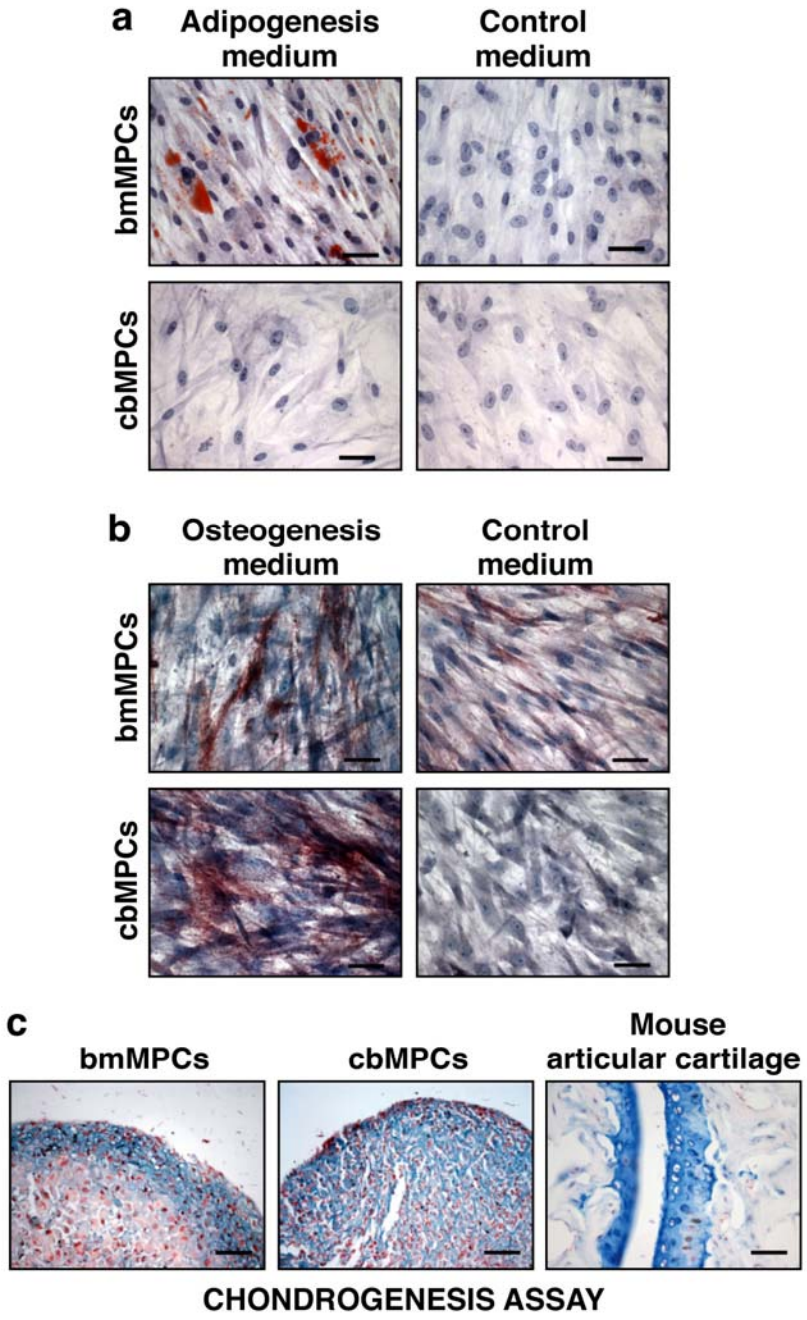

(a) Differentiation into adipocytes was assessed by Oil Red O staining, and it was evident in bmMPCs, but absent in cbMPCs. (b) bmMPCs and cbMPCs differentiation into osteocytes was revealed by alkaline phosphatase staining. (c) bmMPCs and cbMPCs differentiation into chondrocytes was revealed by the presence of glycosaminoglycans, detected by Alcian Blue staining. Sections of mouse articular cartilage served as control (scale bars, 50 μm).

Supplementary Figure 5. PDGF-Rβ expression on MPCs

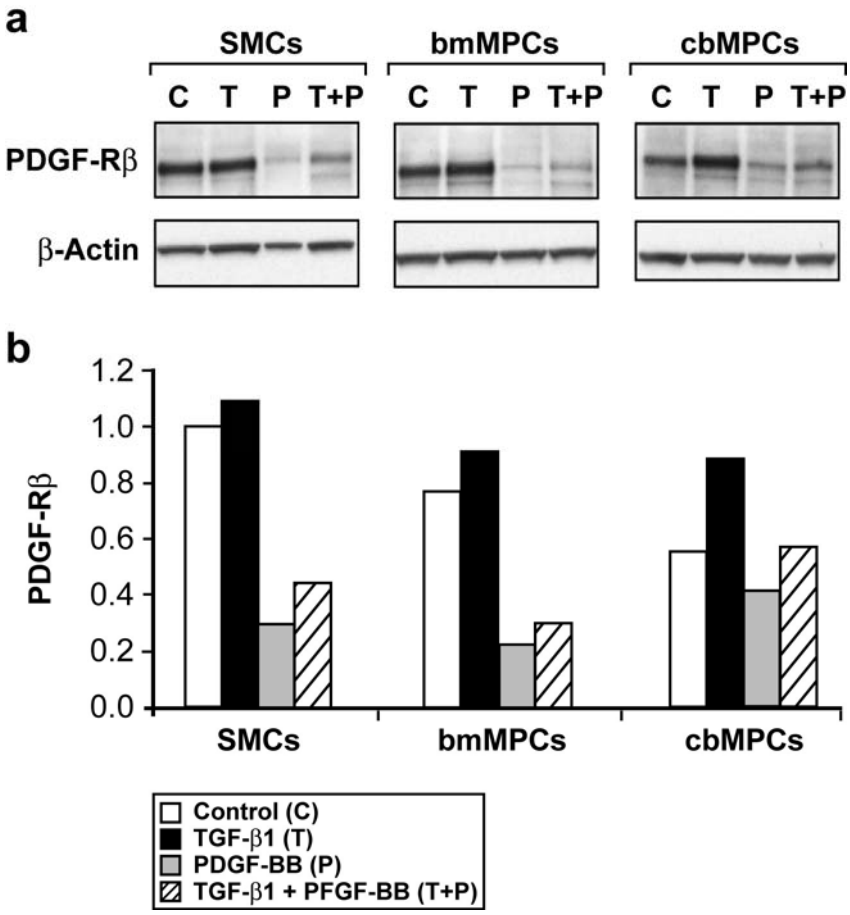

(a) Both bmMPCs and cbMPCs expressed PDGF-Rβ in culture. Similarly to SMCs, PDGF-Rβ expression was up-regulated by TGF-β1 and down-regulated by PDFG-BB. (b) Quantification was performed by image analysis of the bands. SMCs obtained from human sapheneous vein served as control.

Supplementary Figure 6. Differentiation of MPCs into smooth muscle cells

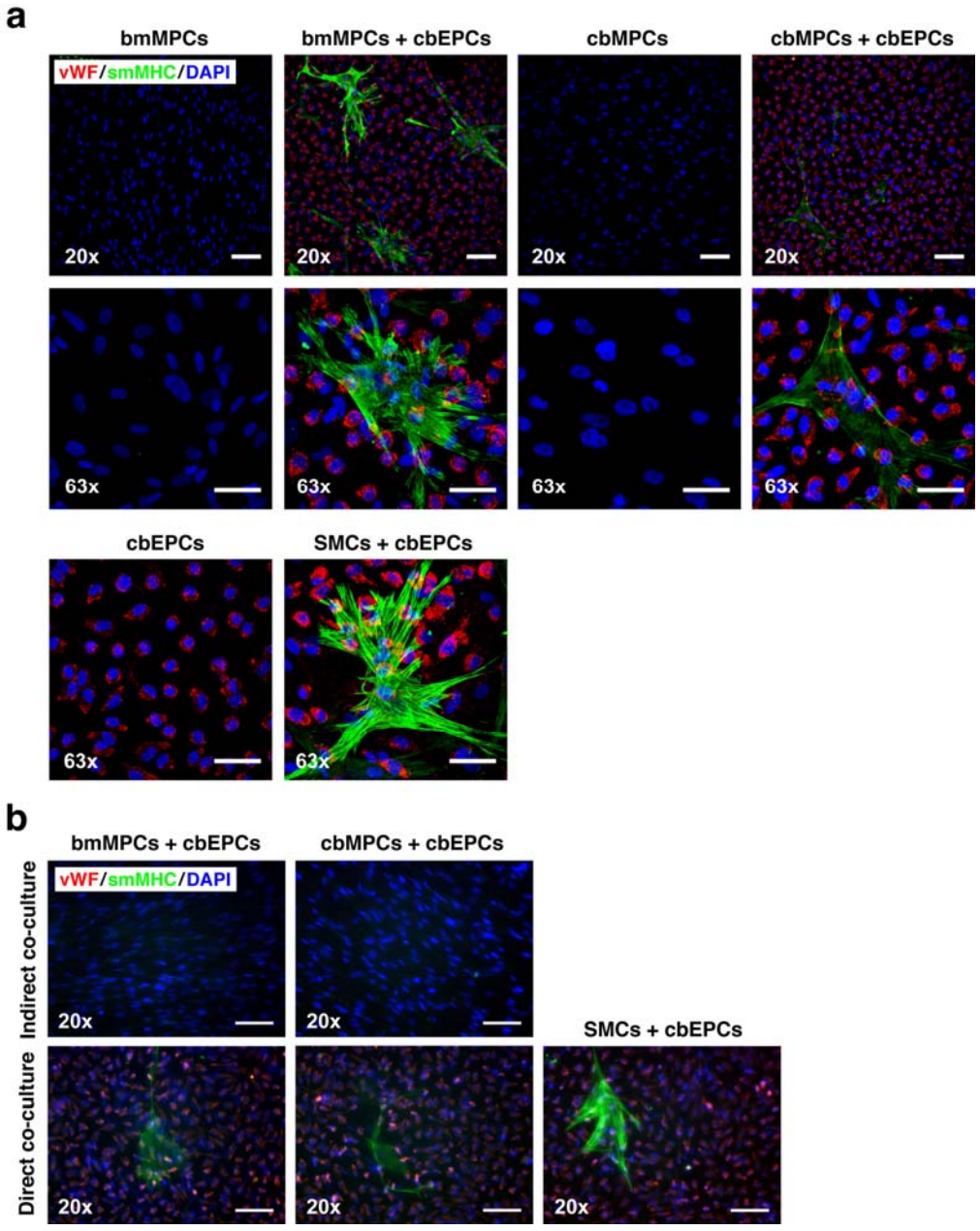

(a) Induction of SMC phenotype was assessed by the expression of smMHC. Immunofluorescence staining with anti-vWF-Texas-Red and anti-smMHC-FITC, as well as nuclear staining with DAPI, revealed that smMHC was absent in both bmMPCs and cbMPCs, but it was induced in MPCs when co-cultured with cbEPCs (1:1 EPCs to MPCs ratio) for 7 days in EPC-medium. (b) Importantly, smMHC induction did not occur when MPCs were indirectly co-cultured with cbEPCs using a Transwell culture system. SMCs obtained from human sapheneous vein served as control. 20x and 63x scale bars correspond to 100 µm and 50 µm respectively.

Supplementary Figure 7. Lack of vascularization in implants with Matrigel alone

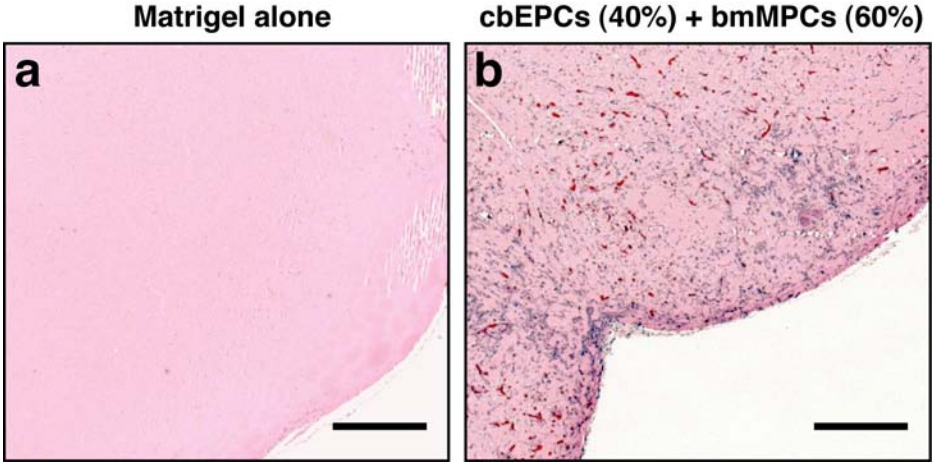

(a) Implants containing only Matrigel were injected subcutaneously on the back of six-week-old nu/nu mice and evaluated after one week. H&E staining showed that Matrigel alone was inert, and implants were devoid of blood vessels. (b) In contrast, Matrigel implants containing 40% cbEPCs and 60% bmMPCs showed an uniform and extensive presence of lumenal structures containing murine erythrocytes throughout the implants (scale bars, 500 µm).

Supplementary Figure 8. *In vitro* secretion of VEGF

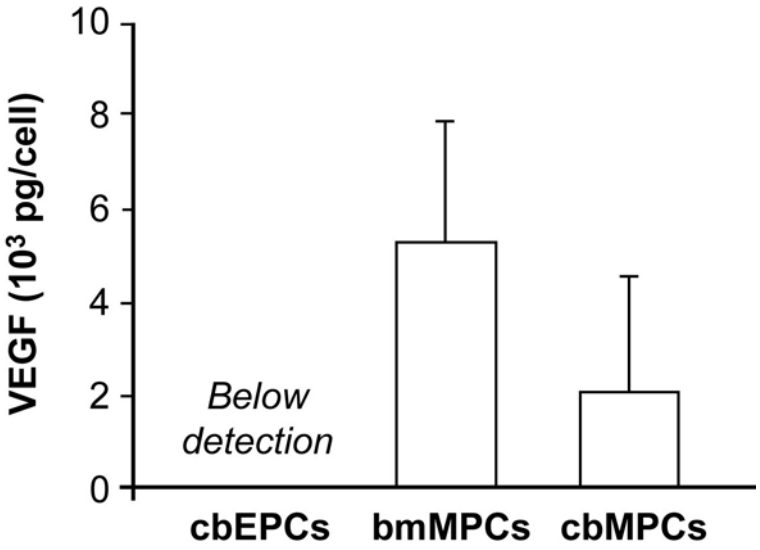

Both bmMPCs and cbMPCs secreted significant more VEGF *in vitro* than cbEPCs. Quantitative measurement of human VEGF in the cell culture supernatant was carried out using a Quantikine ELISA kit, and VEGF values were normalized to total cell number determined at the time of supernatant collection.

Supplementary Figure 9. Human specific CD31-positive lumens forming the engineered vascular networks

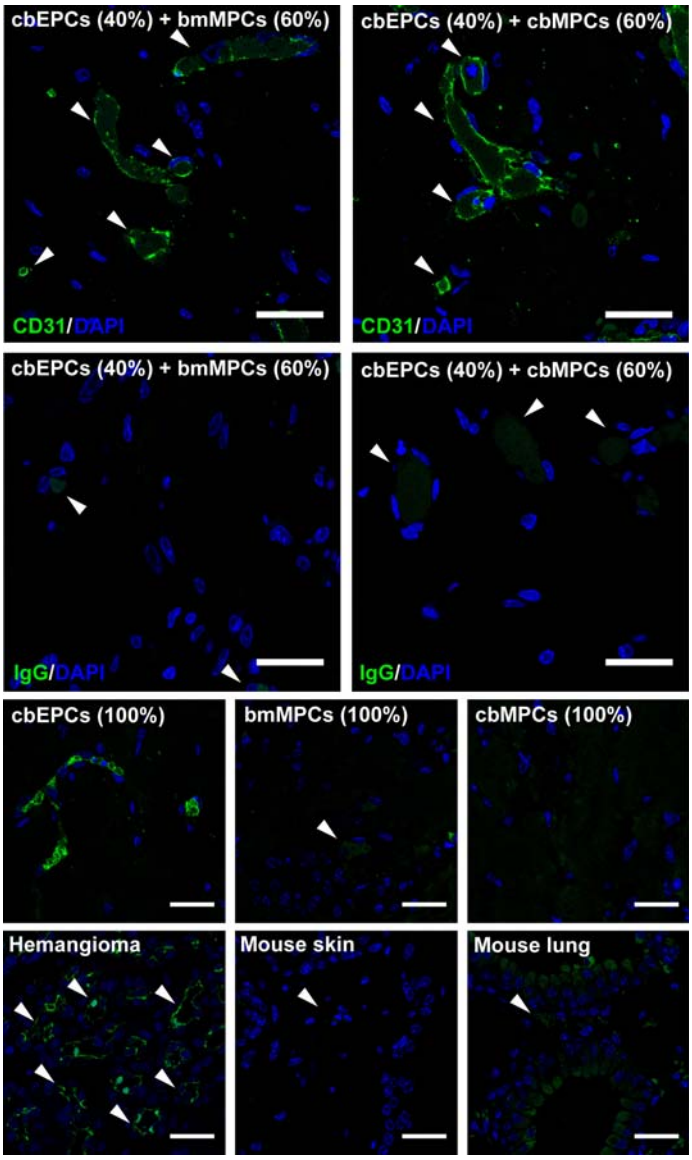

Matrigel implants containing 40% cbEPCs and 60% MPCs (either bmMPCs or cbMPCs) were injected subcutaneously on the back of six-week-old nu/nu mice. After one week, numerous blood vessels emerged in the implants. These luminal structures were positive for human CD31 (mouse IgG antibodies were used for control), confirming the lumens were lined by the implanted cells. Human CD31-expressing cells were observed in implants with cbEPCs alone, but these cells failed to form microvessels after one week. Implants with only MPCs presented infiltration of murine blood capillaries that were negative for human CD31. Human infantile hemangioma (human CD31-positive vessels), and mouse skin and lung (human CD31-negative vessels) served as control tissues. White arrow heads indicate blood vessels. All scale bars correspond to 30 µm.

Supplementary Figure 10. Cellularity stabilization on the Matrigel implants

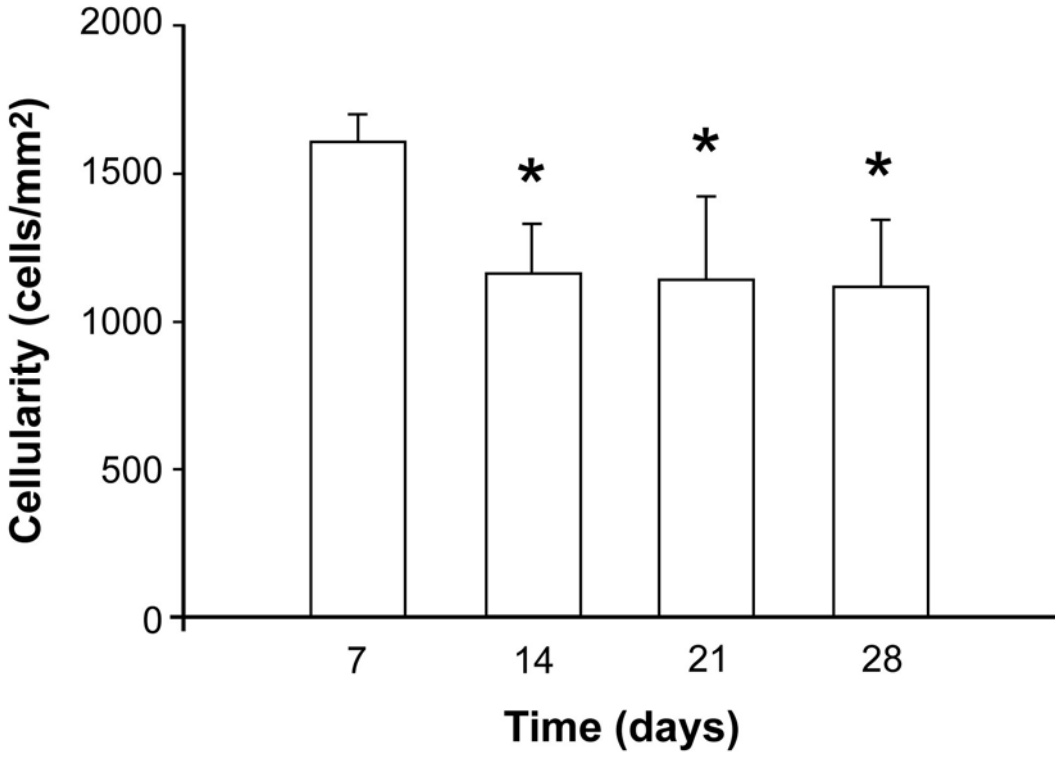

Matrigel implants containing 40% cbEPCs and 60% bmMPCs were injected subcutaneously on the back of six-week-old nu/nu mice and cellularity analyzed at 7, 14, 21, and 28 days. The total number of cells within the Matrigel implants decreased from day 7 to day 14 and stabilized then after. Values reported correspond to the average cellularity expressed as cells/mm^2 ± S.D. obtained from four individual mice. * $P < .05$ compared to implants at day 7 (n=4).

Supplementary Figure 11. Presence of adipocytes in the Matrigel implants

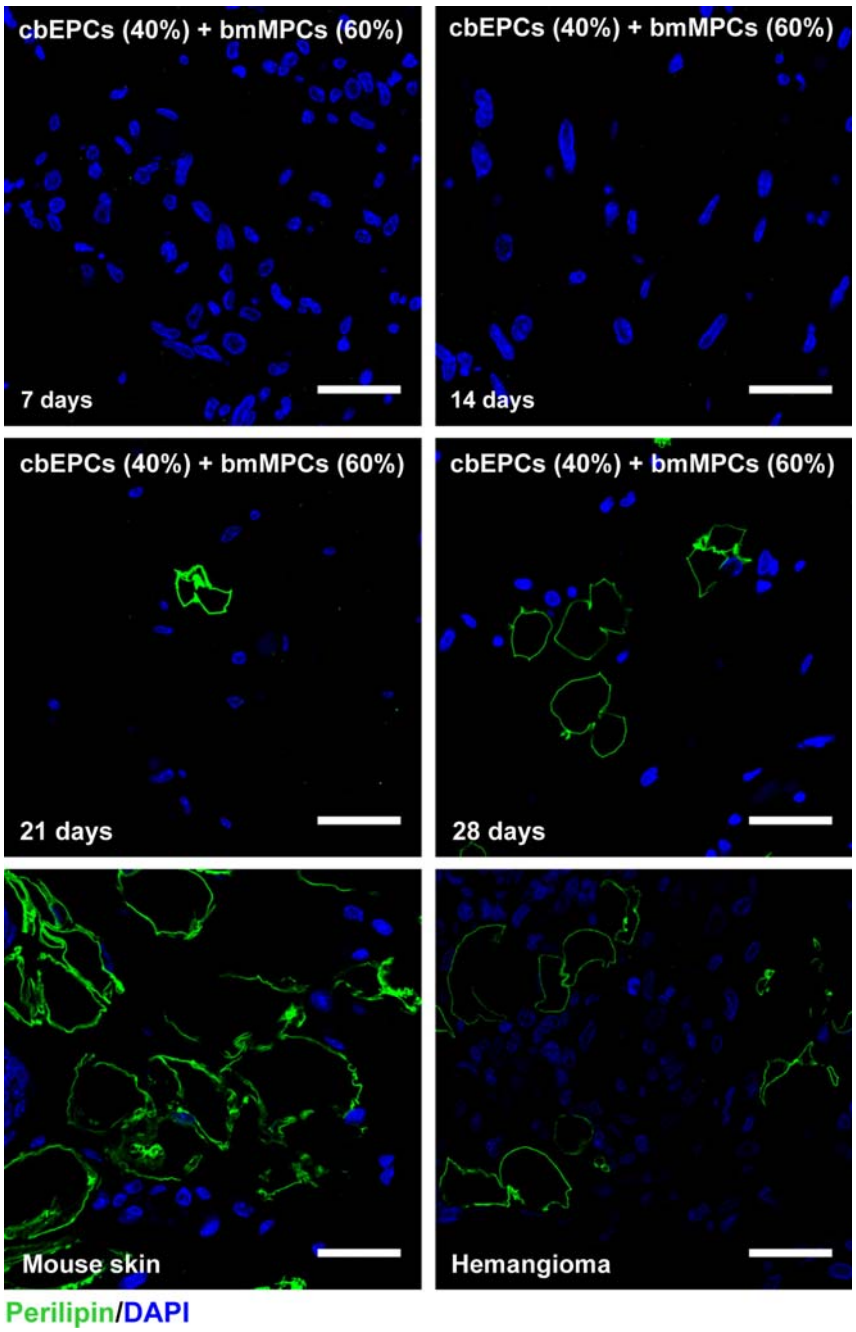

Matrigel implants containing 40% cbEPCs and 60% bmMPCs were injected subcutaneously on the back of six-week-old nu/nu mice and the presence of perilipin-positive adipocytes was assessed at 7, 14, 21, and 28 days. Immunofluorescence staining with anti-perilipin-FITC and nuclear staining with DAPI, revealed the low-to-moderate presence of adipocytes after 21 and 28 days. No adipocytes were detected before 21 days. Human infantile hemangioma, and mouse skin served as control tissues. All scale bars correspond to 30 μm.

Supplementary Figure 12. Characterization of abEPCs

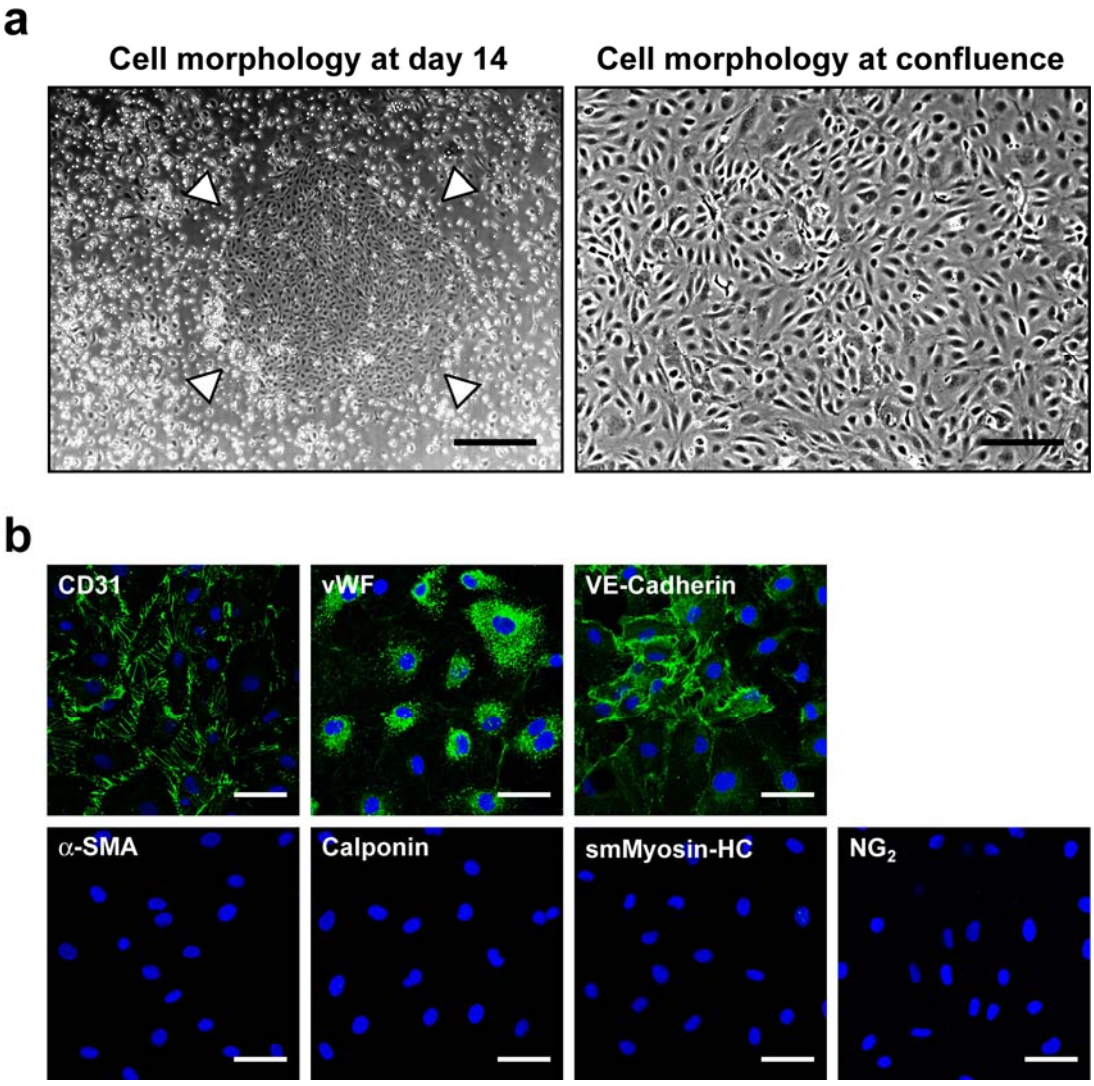

(a) Two-to-three weeks after isolation, abEPCs emerged forming typical EC colonies (scale bar, 500 µm). At confluence, abEPCs presented typical cobblestone morphology (scale bar, 200 µm). (b) abEPCs expressed endothelial markers CD31, vWF, and VE-Cadherin, but were negative for perivascular markers α-SMA, calponin, smMyosin-HC, and NG_2 as determined by indirect immunofluorescence (scale bars, 50 µm).